

VTT

SQUID applications

EASISchool 3, Genova, Italy

Mikko Kiviranta

05/10/2020

1

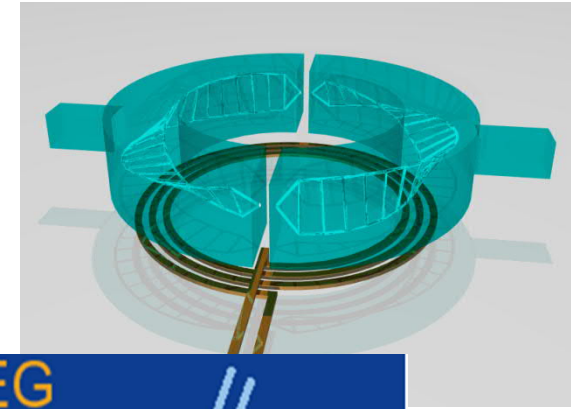
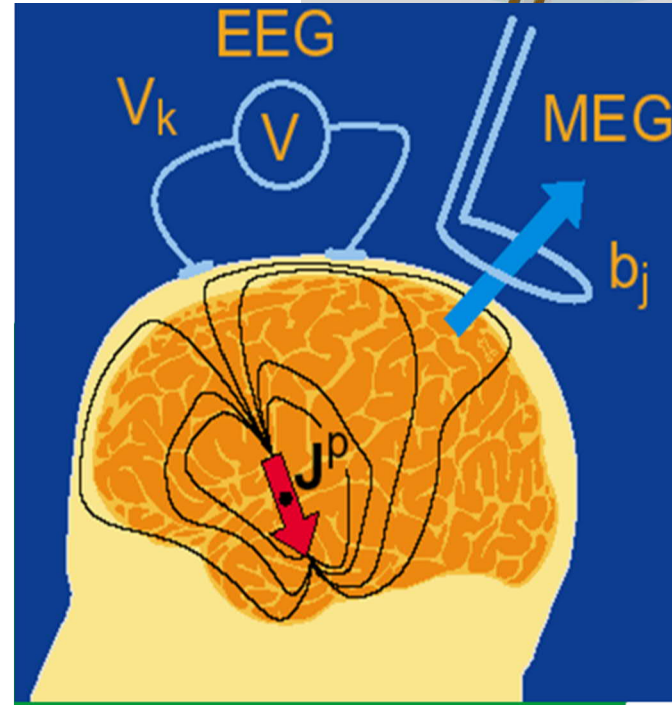
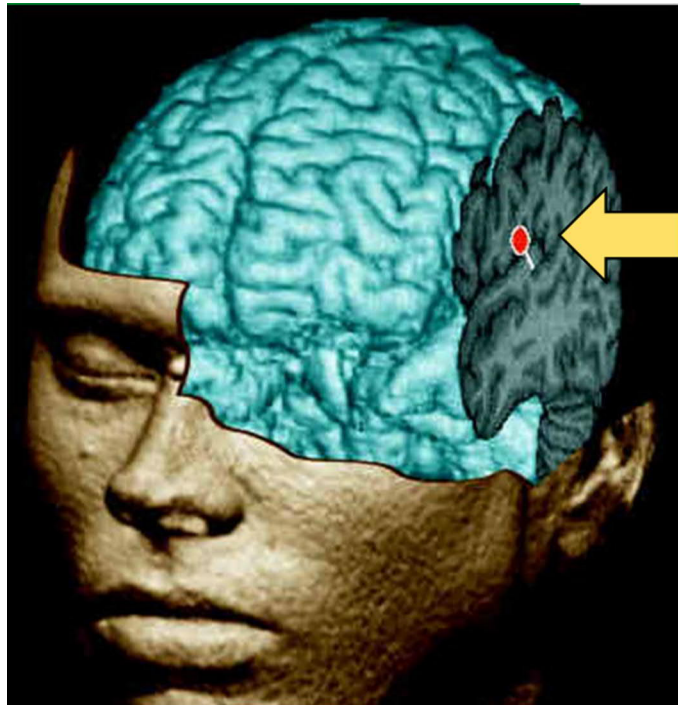
Overview

- Magnetoencephalography
- Ultra-low field Magnetic Resonance Imaging
- Geomagnetism
- Multiplexing Transition Edge Sensors
- A few more exotic applications

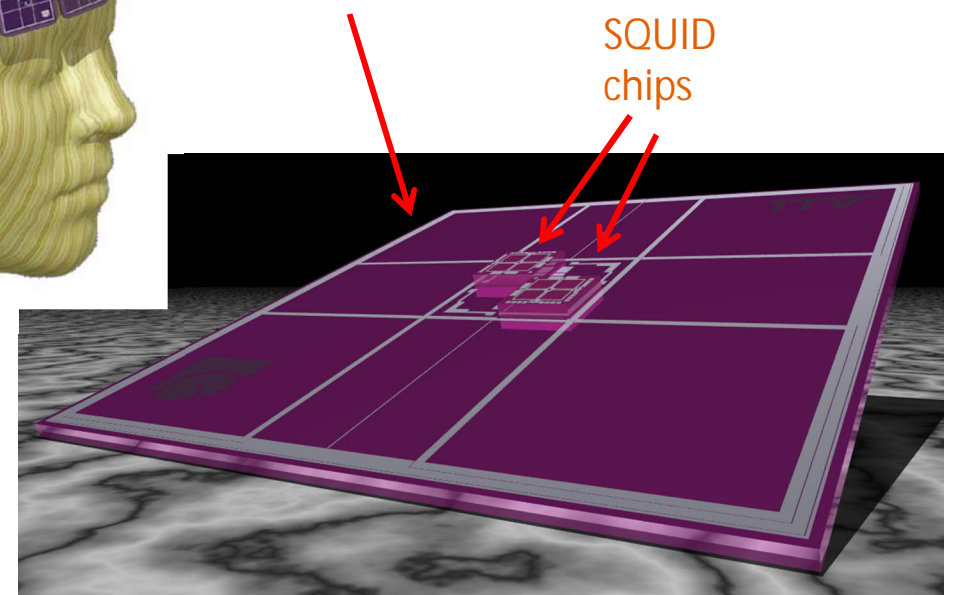
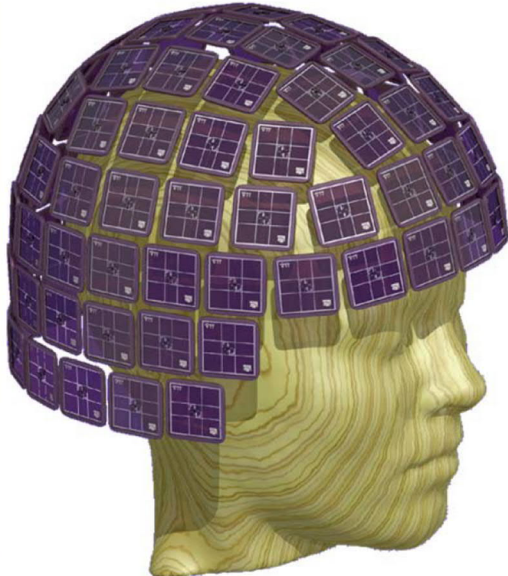


Magnetoencephalography

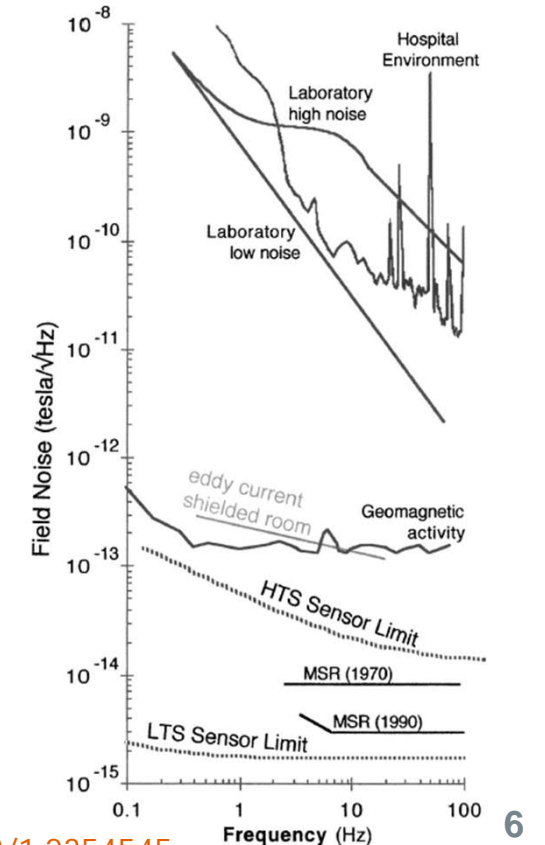
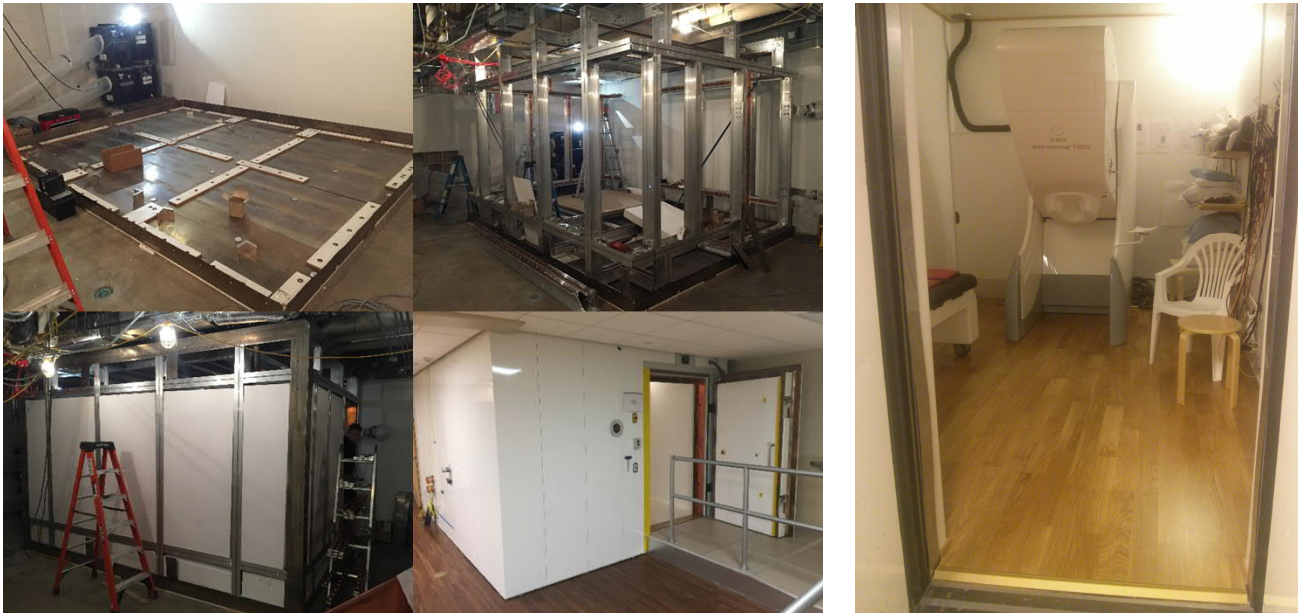
Magnetoencephalography (MEG)



Magnetoencephalography (MEG)



MEG - magnetically shielded rooms



Doi: 10.1063/1.2354545

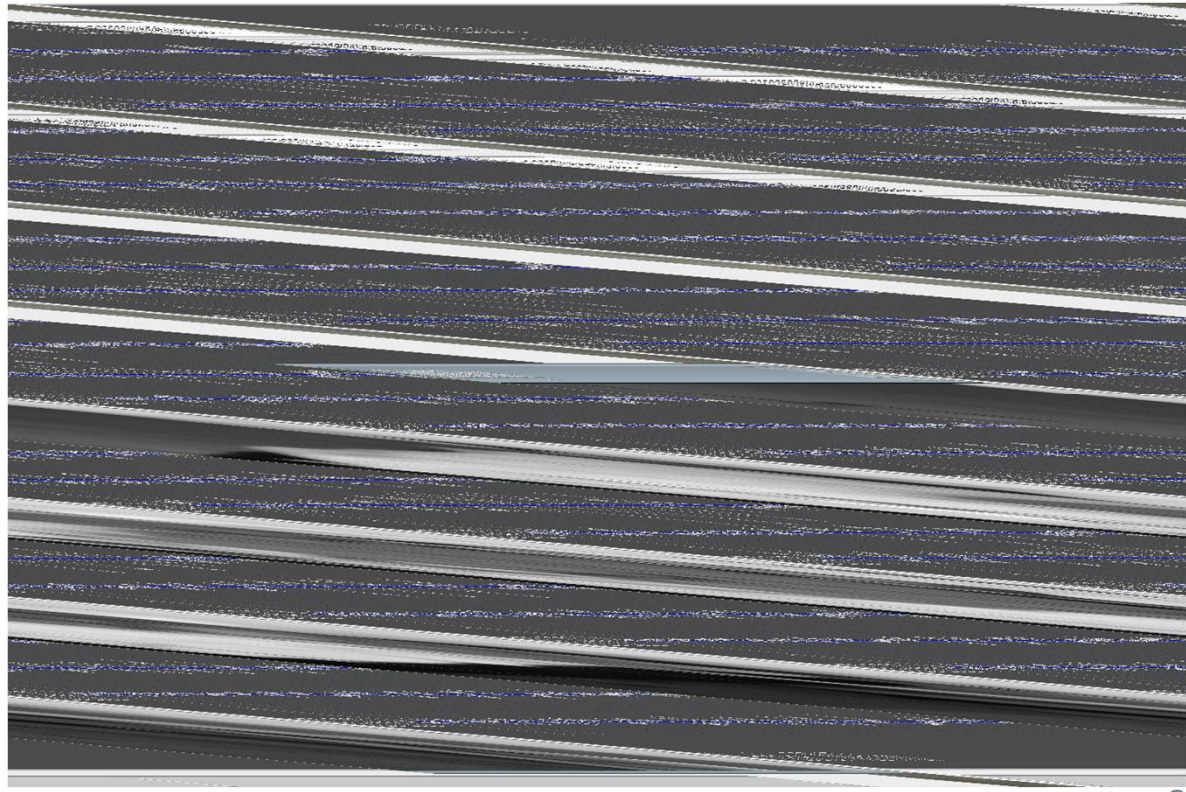
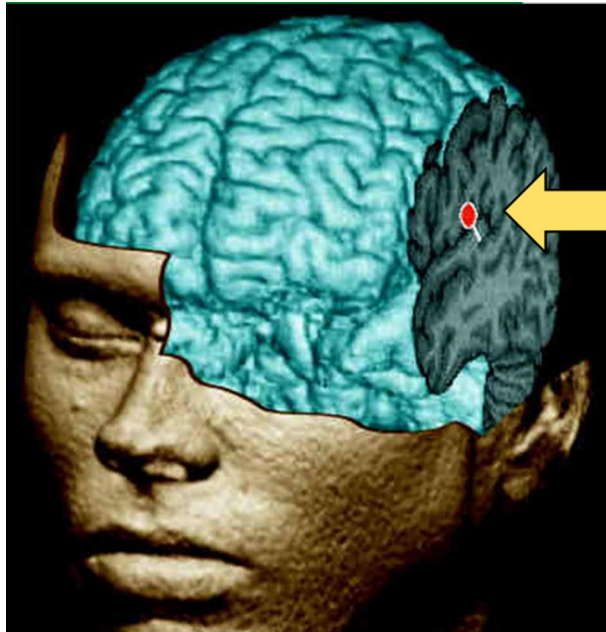
VTT

Full MEGIN system



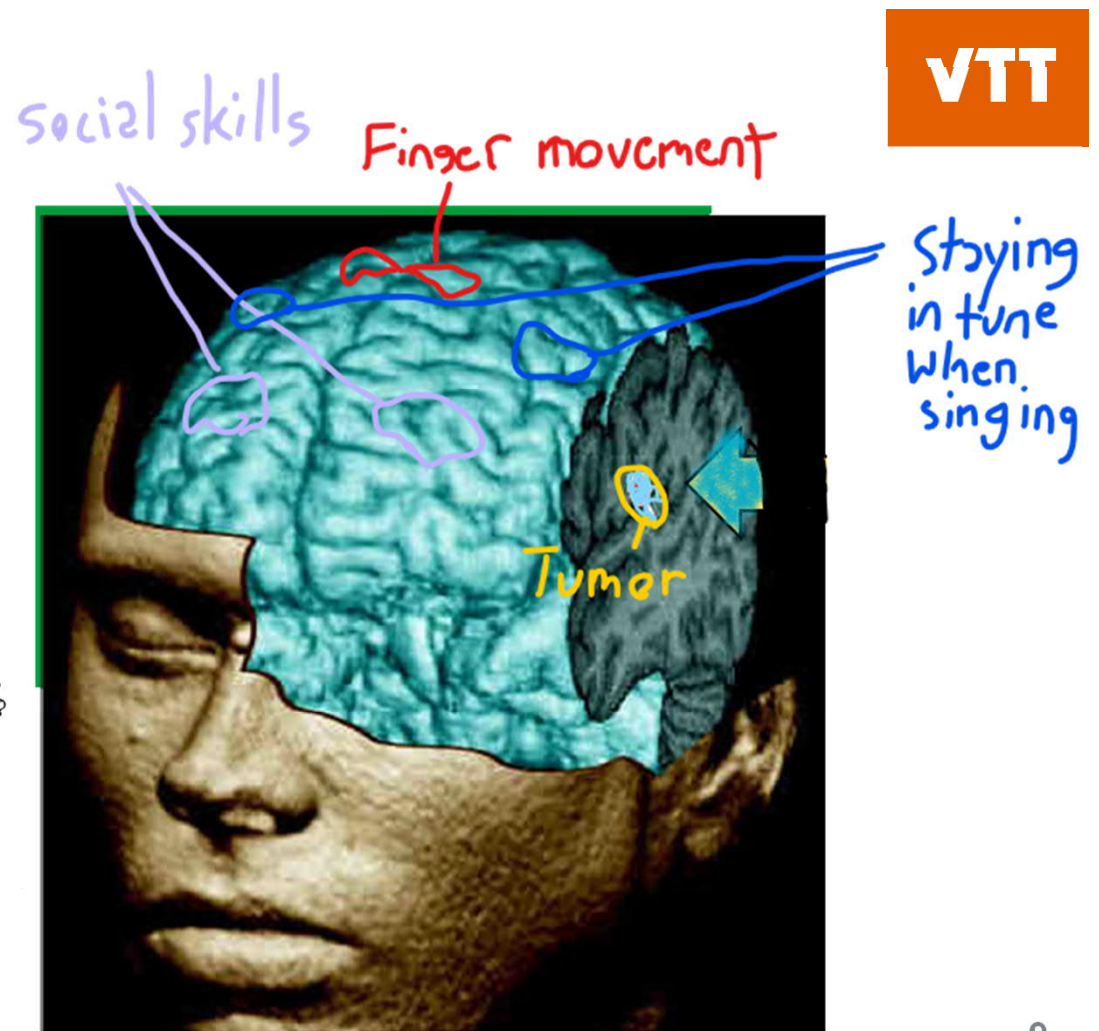
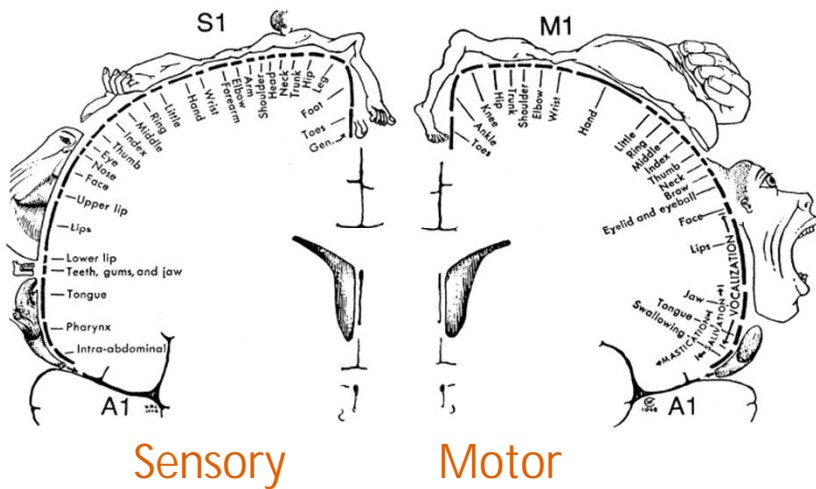
Youtube: pYJW-J_IcC4

MEG applications: epilepsy

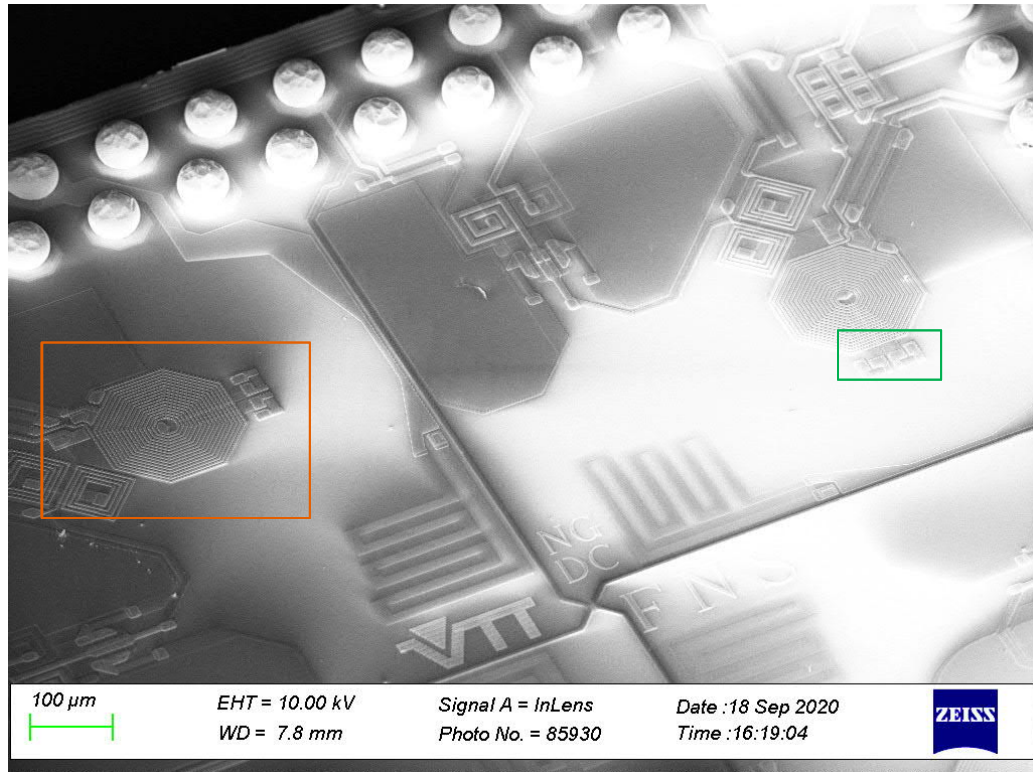


Video:
[doi:10.1016/j.epilepsyres.2013.02.017](https://doi.org/10.1016/j.epilepsyres.2013.02.017)

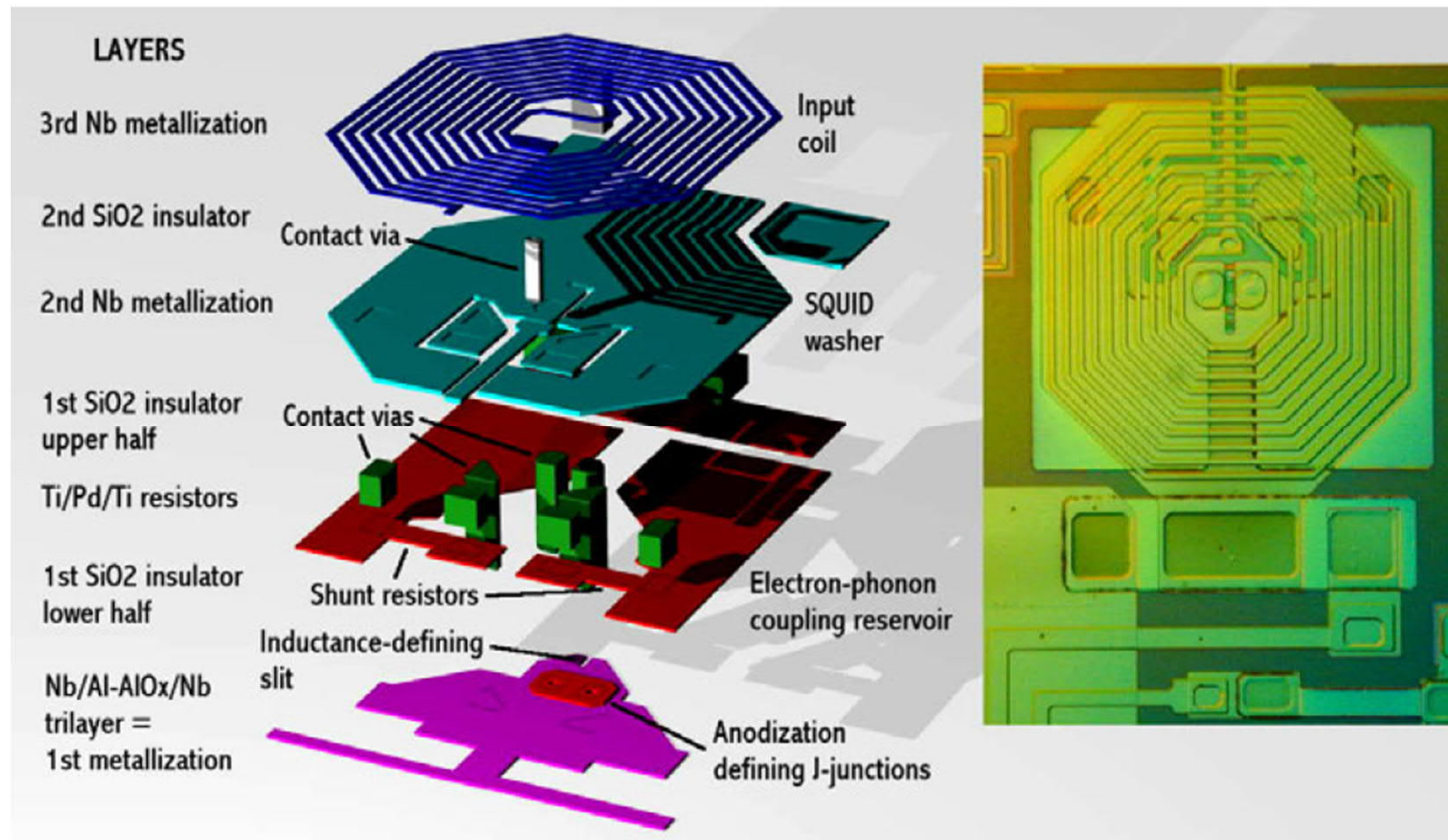
MEG applications: Neurosurgery planning



An actual SQUID magnetometer chip



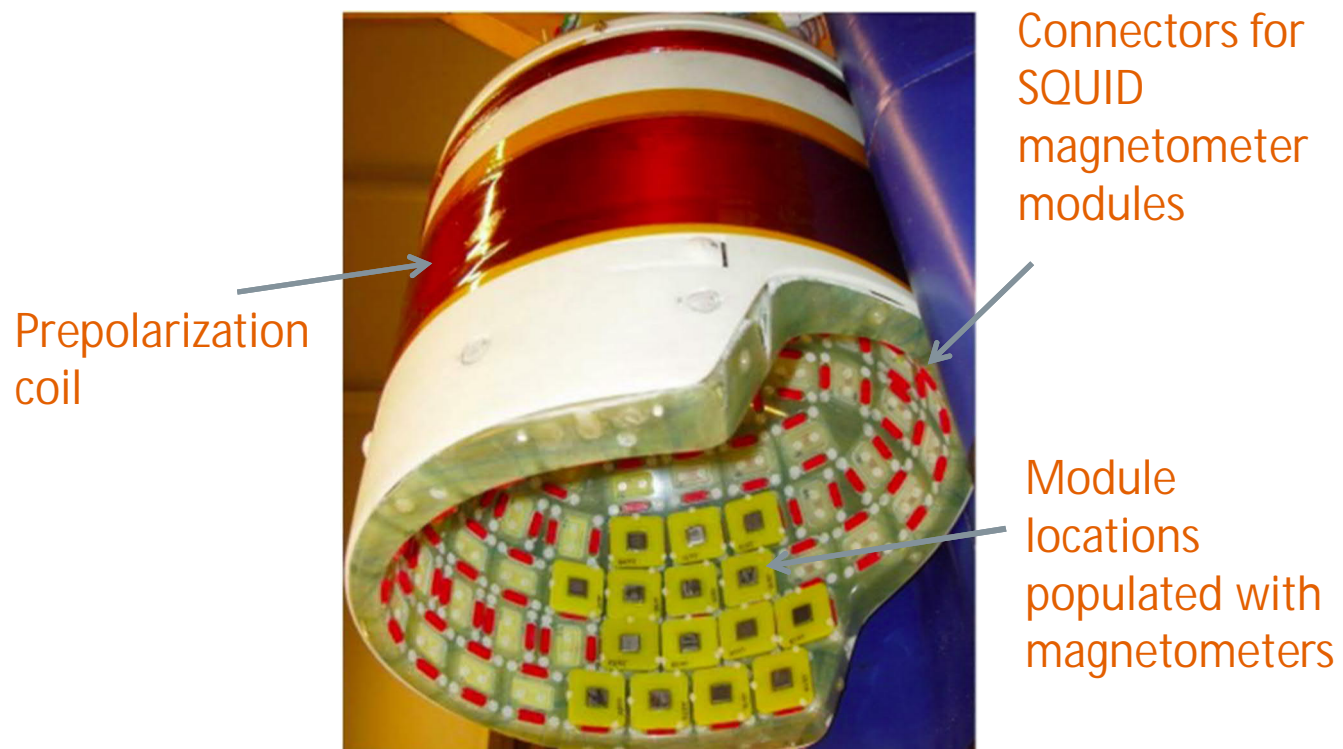
Typical thin film fabrication stack





Ultra low field Magnetic Resonance Imaging

Ultra low field Magnetic Resonance Imaging ULF-MRI

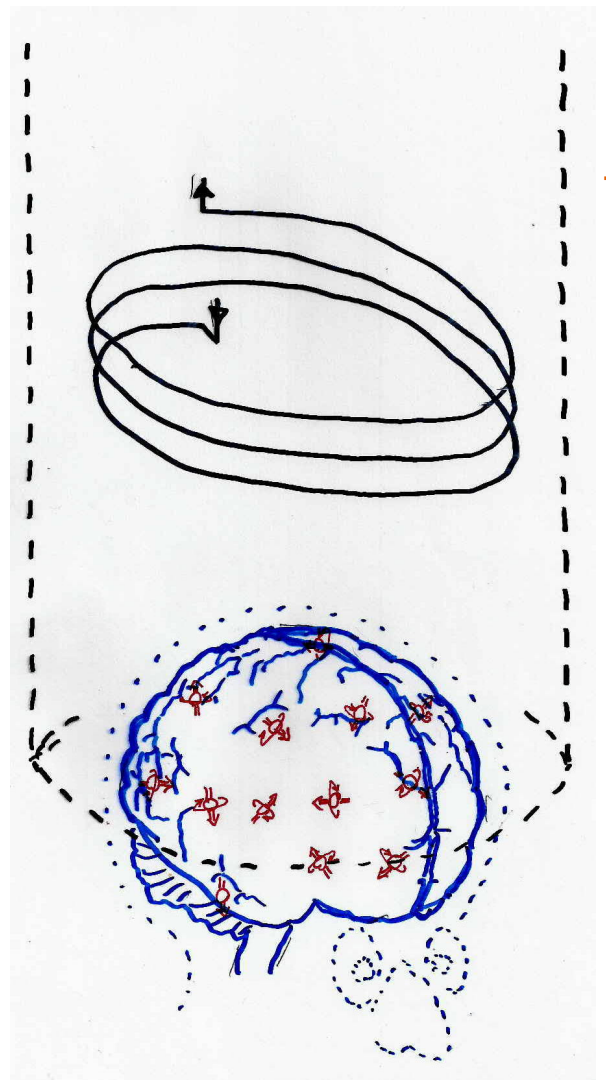


ULF-MRI



Magnetic moments of hydrogen nuclei (water)

Randomly oriented



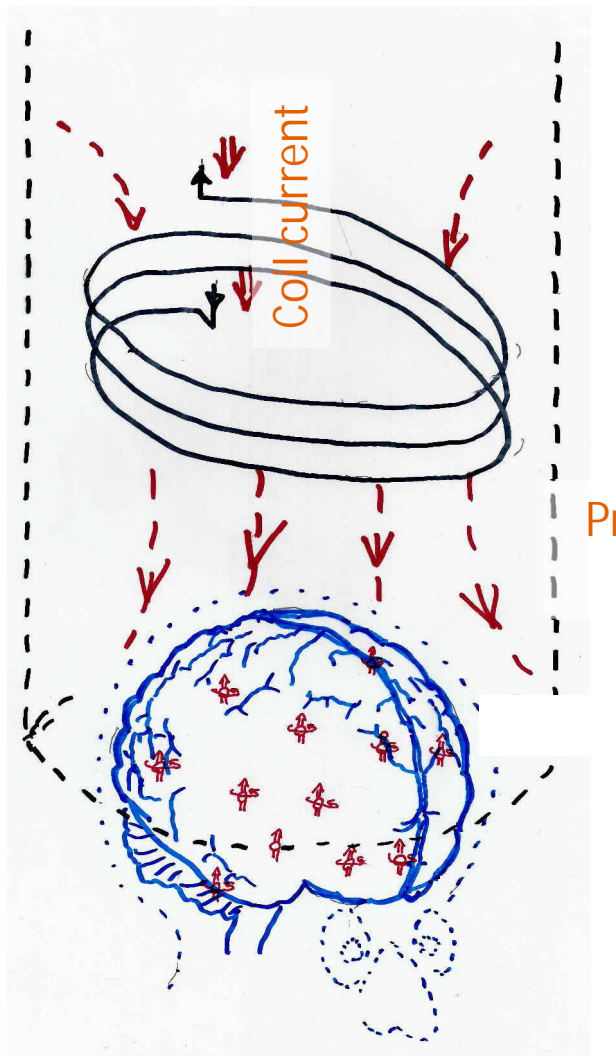
Liquid helium vessel

ULF-MRI

Prepolarization field
~100 mT

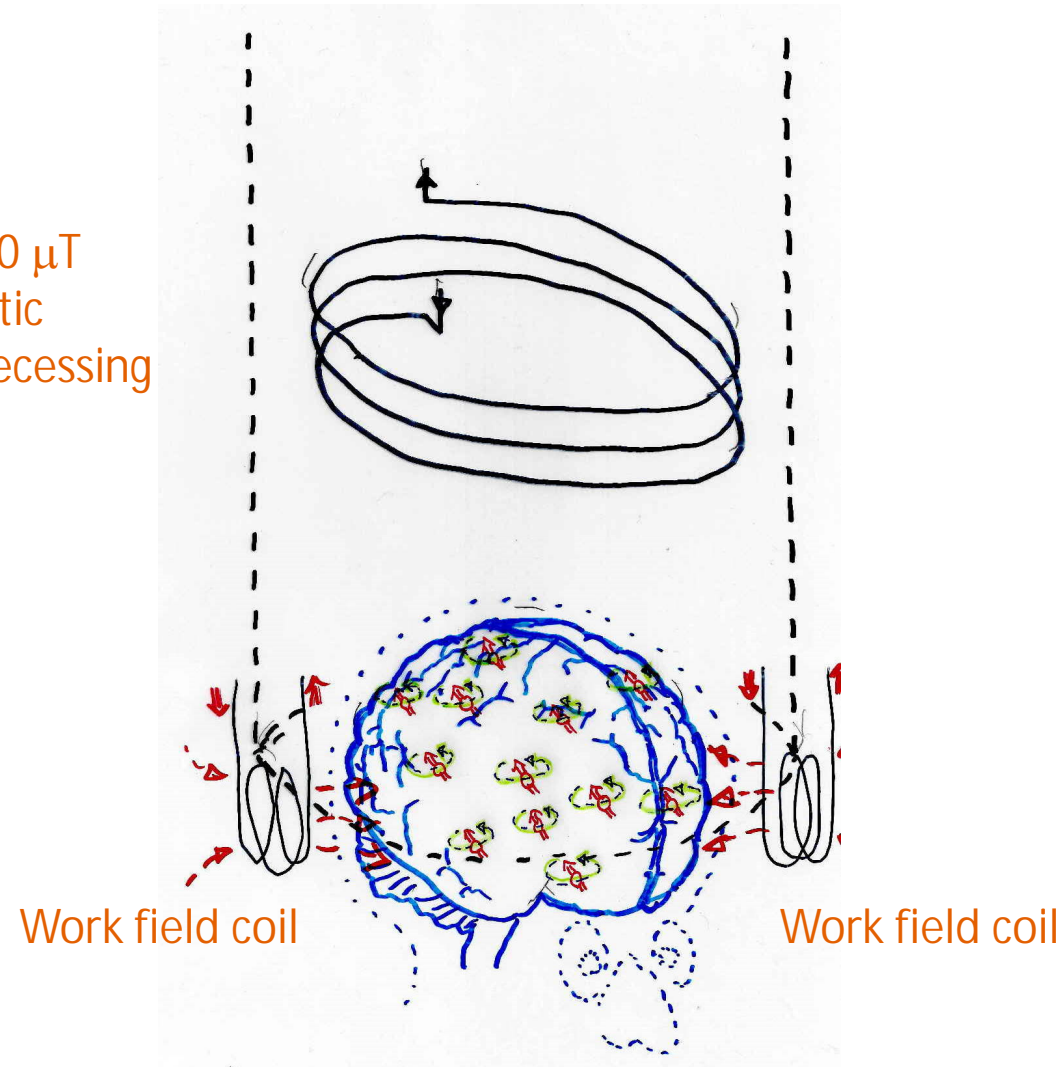
Orients hydrogen nuclei

SQUIDs are dead during this phase



ULF-MRI

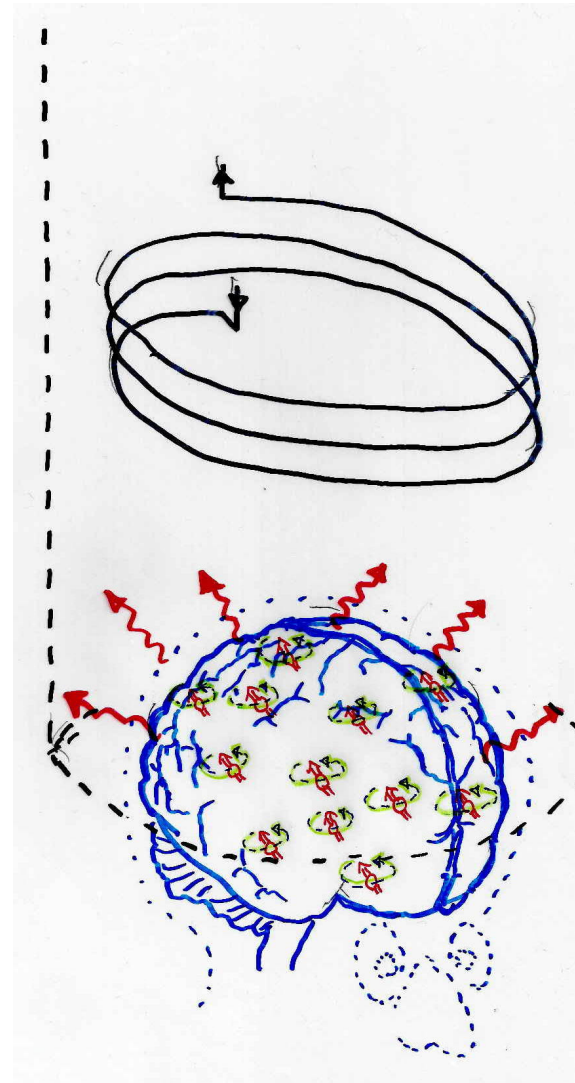
Work field of $\sim 100 \mu\text{T}$
'kicks' the magnetic
momenta into precessing
motion



ULF-MRI

Magnetic momenta performing the precessing motion emit magnetic signal at a few kHz frequency

Precession-generated field ~100 pT



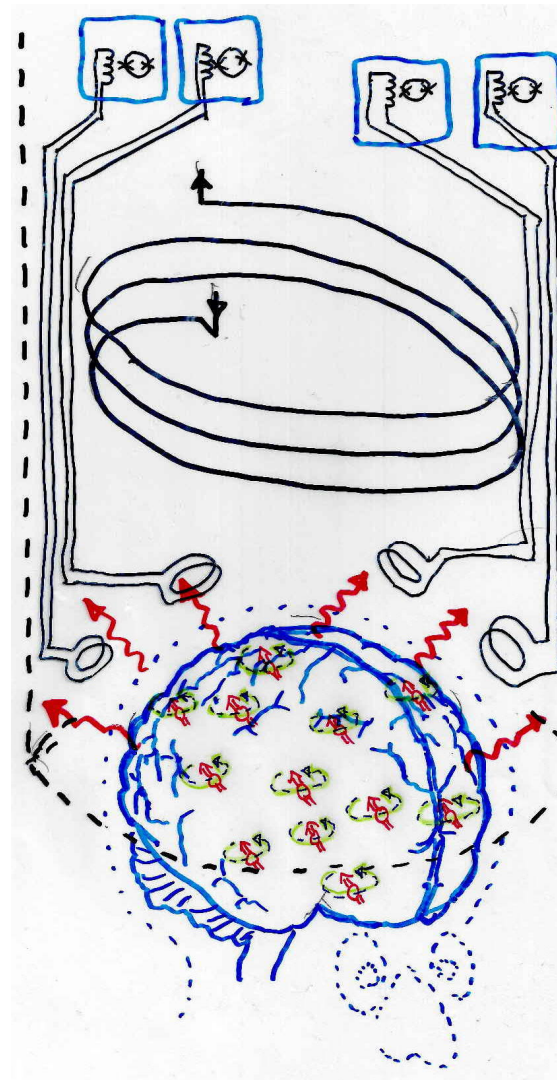
ULF-MRI

Traditional arrangement of SQUIDs in an ultra-low-field MRI

SQUIDs

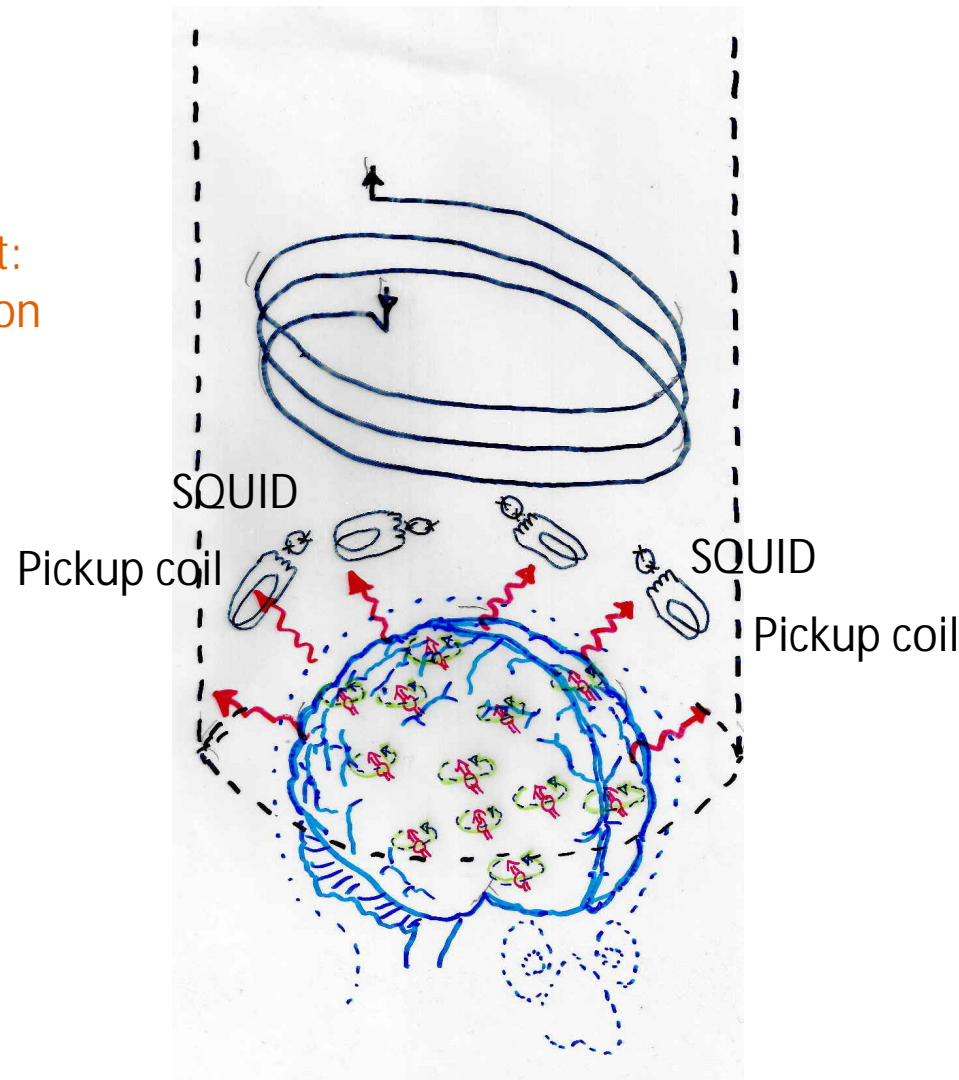
Magnetic shields

VTT



ULF-MRI

New SQUID arrangement:
exposed to prepolarization
field

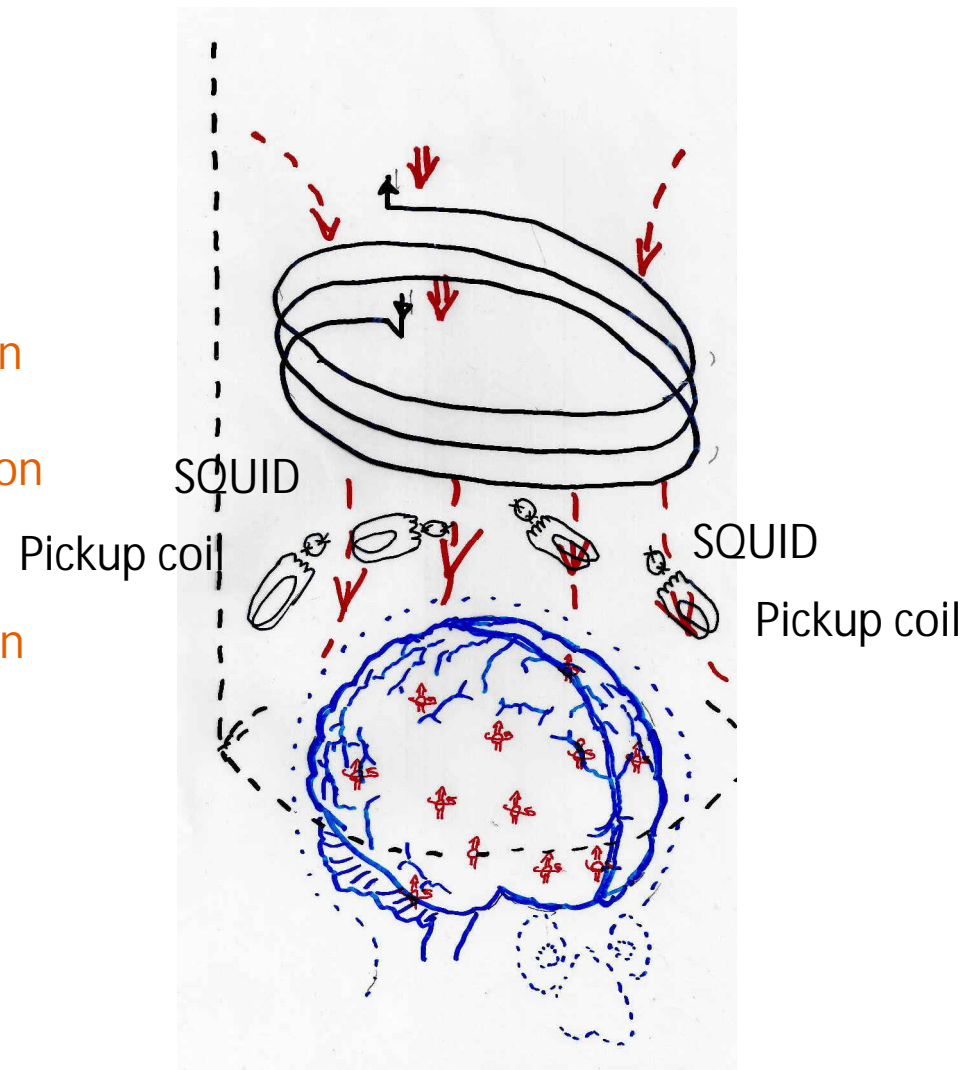


VTT

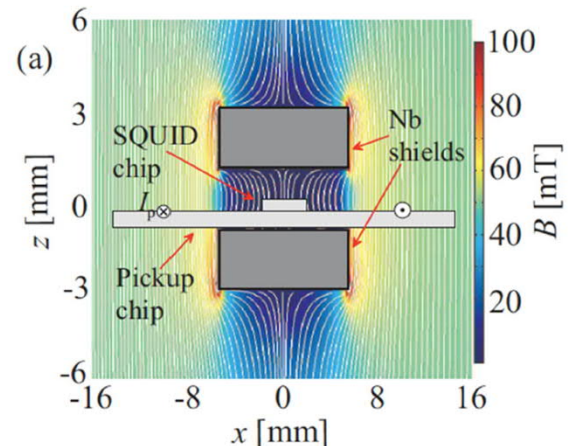
ULF-MRI

Challenge: a few milliseconds before measuring the precession (work) field, SQUIDs are exposed to prepolarization field

Factor of 10^{15} higher than the required field sensitivity!

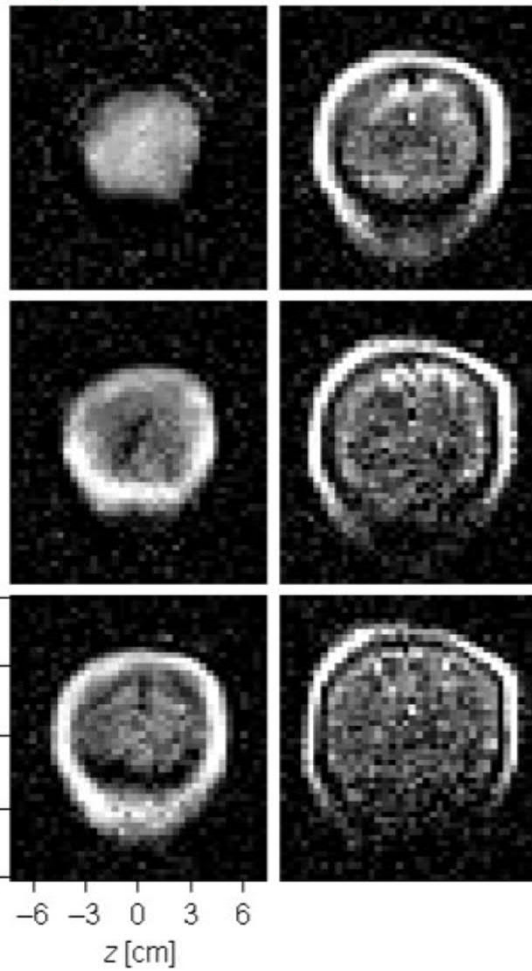


ULF-MRI

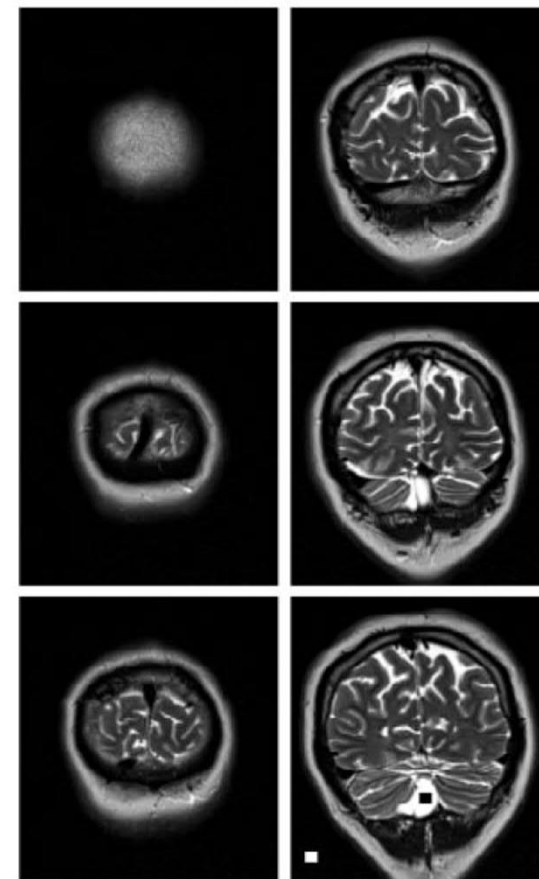


doi:10.1088/0953-2048/24/7/075020

$B_p = 22 \text{ mT}$, $B_0 = 50 \mu\text{T}$



$B_0 = 3 \text{ T}$



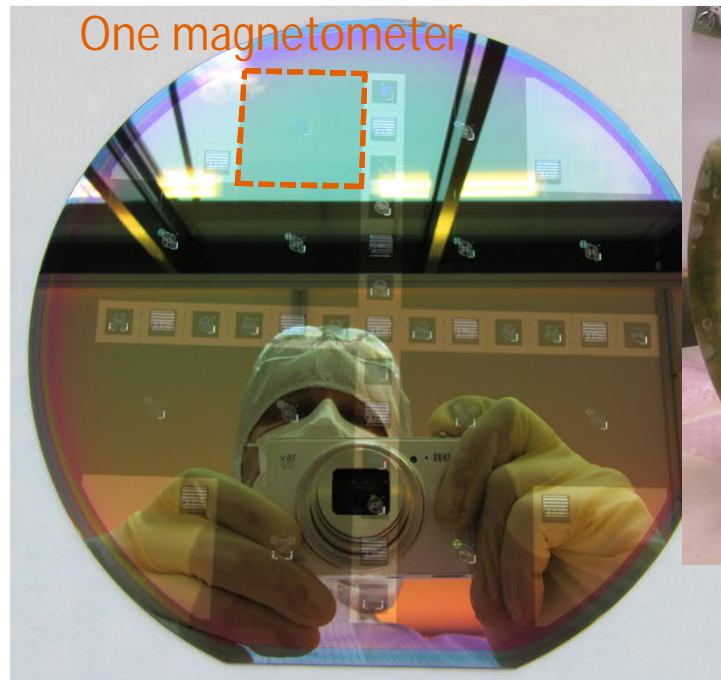
VTT

Doi: 10.1002/mrm.24413

ULF-MRI

New direction:

- SQUID magnetometers which do not need shielding.
- Spontaneous recovery in milliseconds, after 100 mT prepolarization pulse
- Work underway



- Undiced 150mm wafer
- Pickup coil linewidth 3 μm
Too narrow to be visible

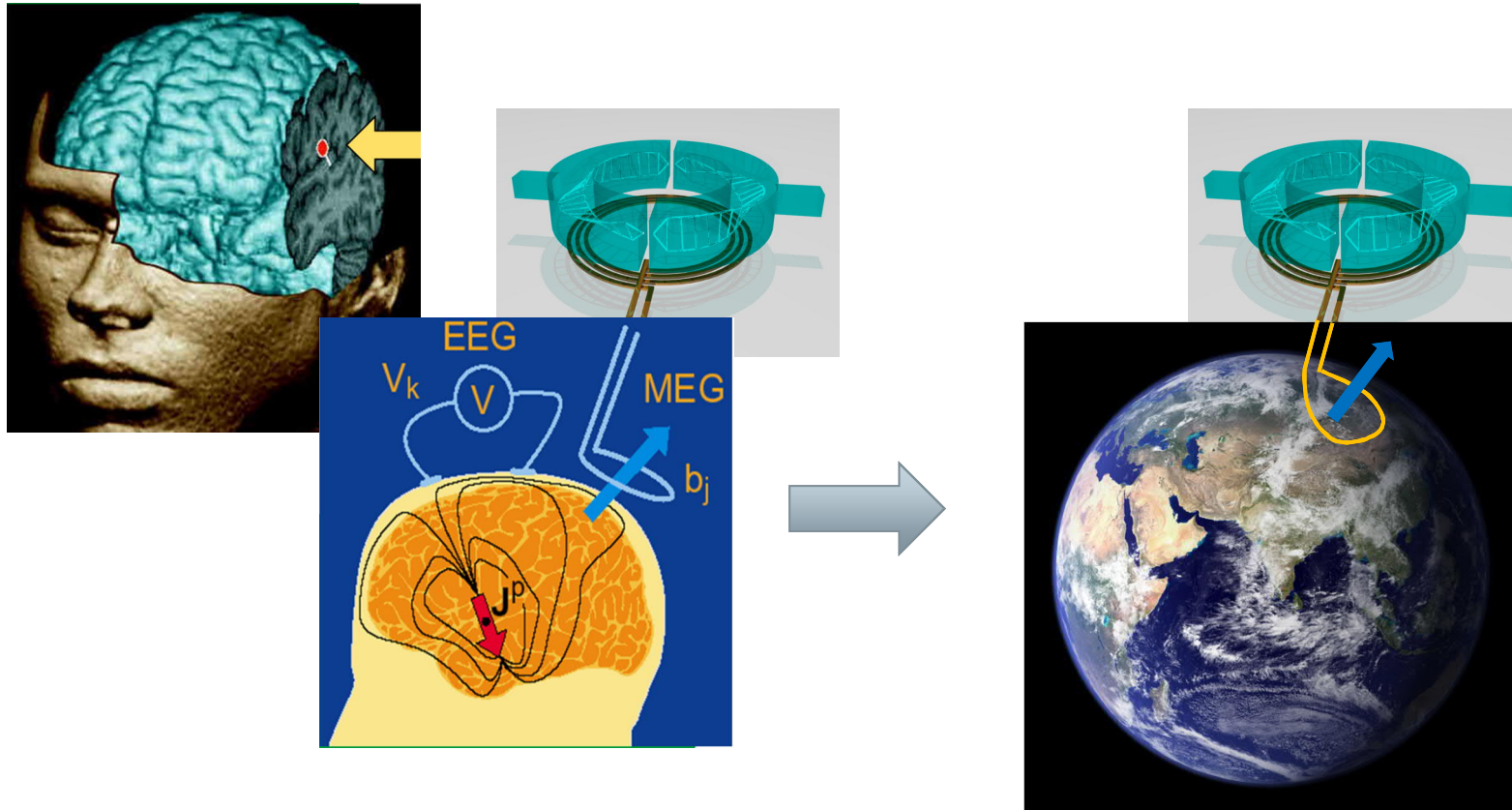


Geomagnetism

Thanks to Ronny Stolz,
Leibniz-institute, Jena

For historical review, see
Doi: 10.1190/1.2133784

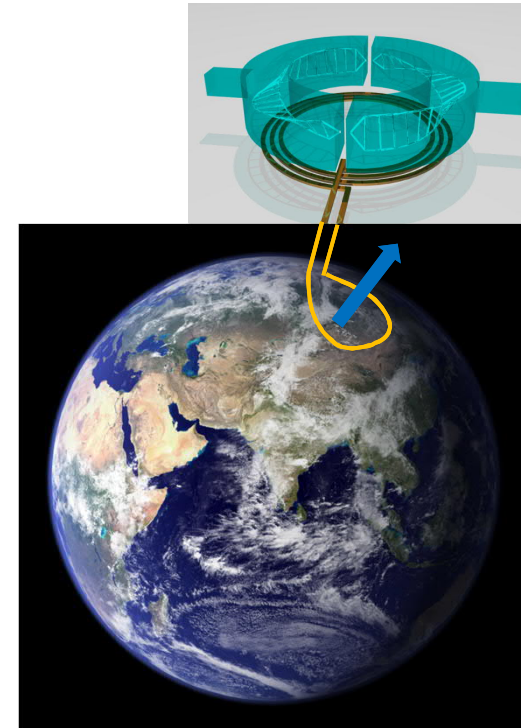
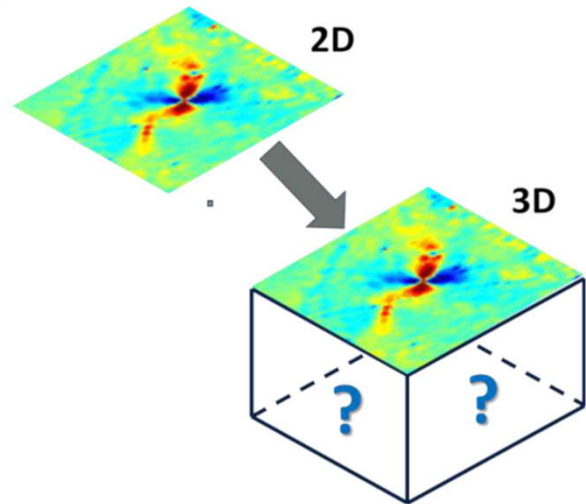
Geomagnetism: similarities with MEG



Geomagnetism: a few methods

Magnetotellurics (MT)

- Passive 'listening' to B-field
- Excited by solar wind – ionosphere interaction
- 3D underground electric conductivity map



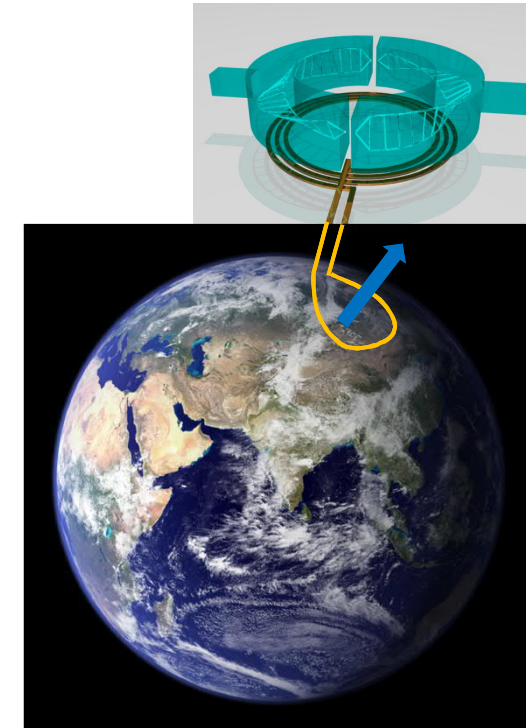
Geomagnetism: a few methods

Magnetotellurics (MT)

- Passive 'listening' to B-field
- Excited by solar wind – ionosphere interaction
- 3D underground electric conductivity map

Magnetic anomaly detection (MAD)

- Passive 'listening' as the magnetometer moves



Geomagnetism: a few methods

Magnetotellurics (MT)

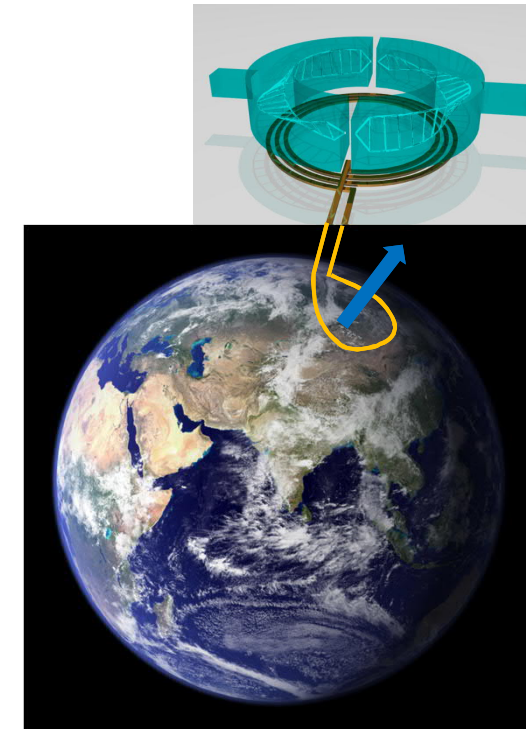
- Passive 'listening' to B-field
- Excited by solar wind – ionosphere interaction
- 3D underground electric conductivity map

Magnetic anomaly detection (MAD)

- Passive 'listening' as the magnetometer moves

Transient electromagnetic pulses (TEM)

- Use coil for active excitation



Geomagnetism: a few methods

Magnetotellurics (MT)

- Passive 'listening' to B-field
- Excited by solar wind – ionosphere interaction
- 3D underground electric conductivity map

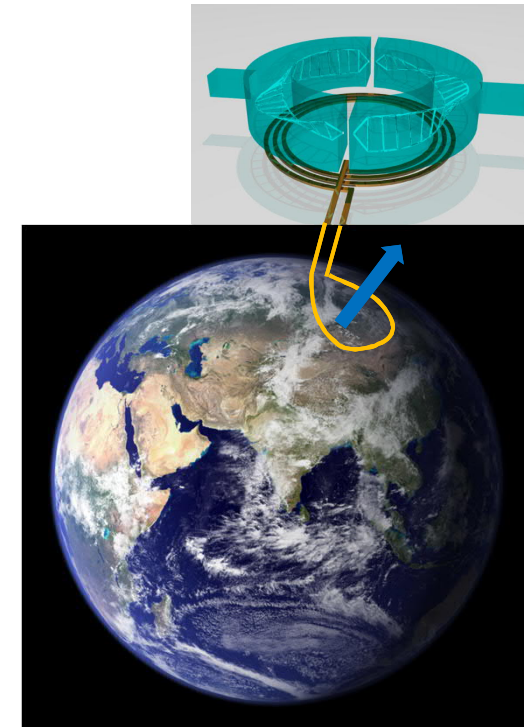
Magnetic anomaly detection (MAD)

- Passive 'listening' as the magnetometer moves

Transient electromagnetic pulses (TEM)

- Use coil for active excitation

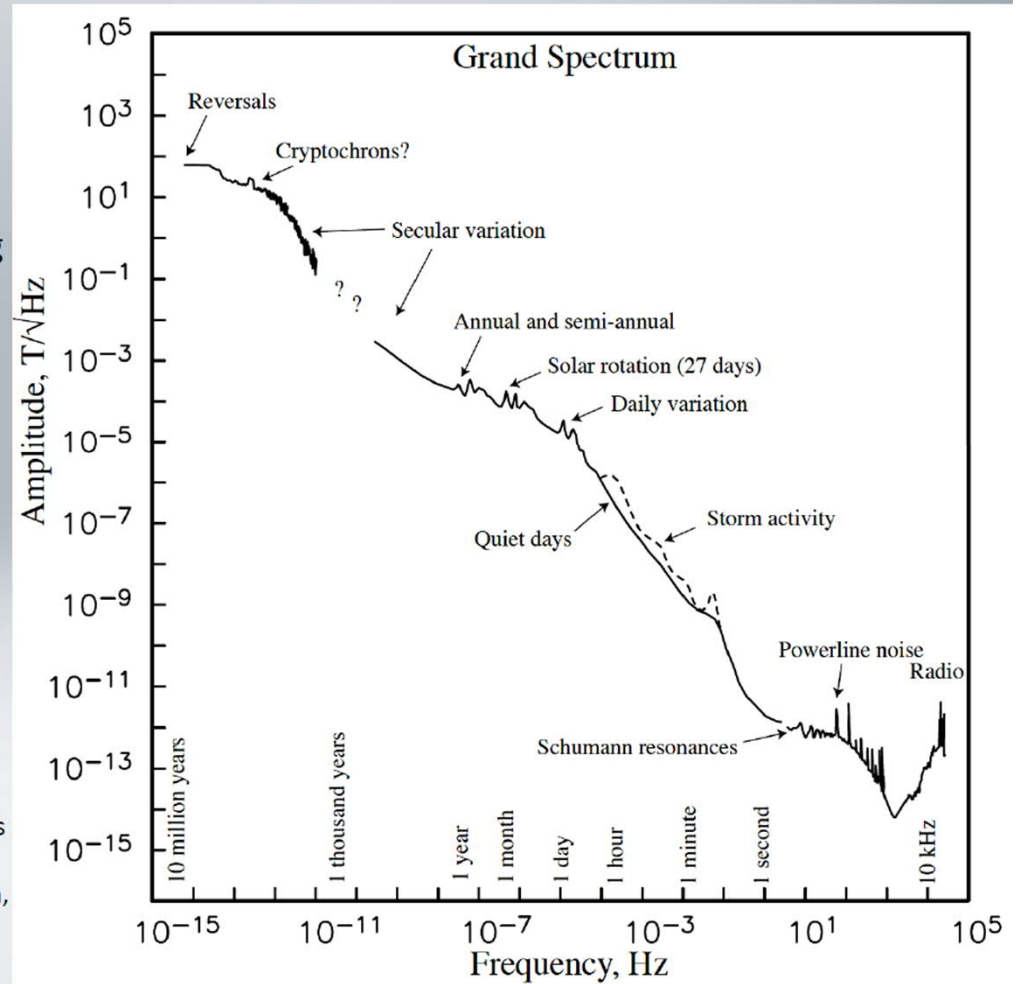
Paleomagnetism, Rock magnetism,
Susceptometry...



Forgacs and Warnick 1967, one of the first SQUID applications

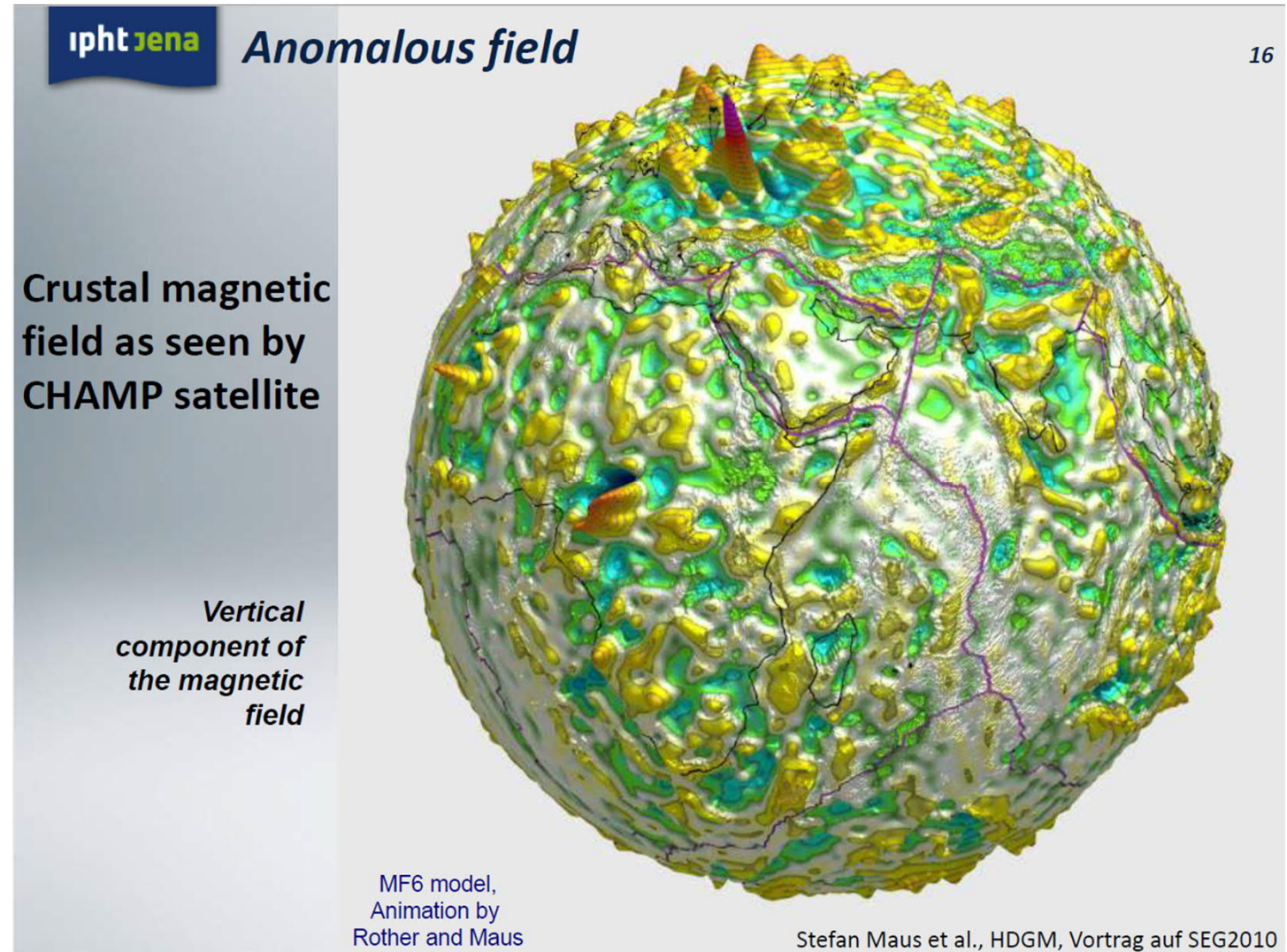
Composed amplitude spectra of geomagnetic variations as function of frequency: label correspond to dominating physical processes with according time scale.

Constable, C.G., & S.C. Constable, 2004. Satellite magnetic field measurements: applications in studying the deep earth. In "The State of the Planet: Frontiers and Challenges in Geophysics", ed. R.S.J. Sparks & C.J. Hawkesworth, AGU. DOI 10.1029/150GM13, pp. 147–160.



Magnetic Anomaly Detection (MAD)

Note the Kursk Magnetic Anomaly and the Iron Mountain of Kiirunavaara (Sweden).
 $\Delta B_{\max} = 190 \mu T$



Magnetic Anomaly Detection (MAD)

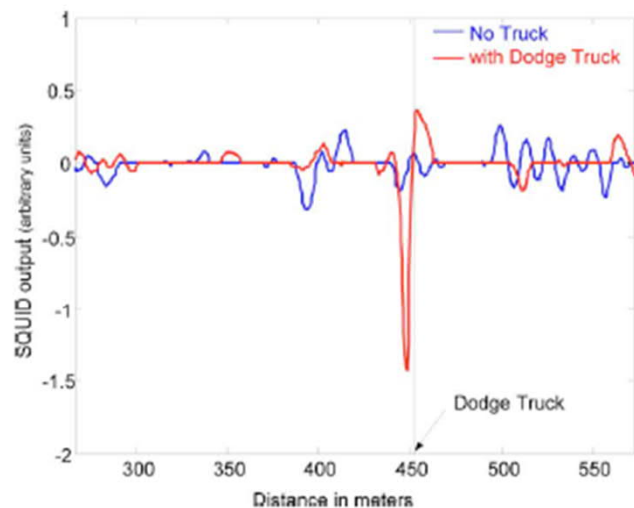
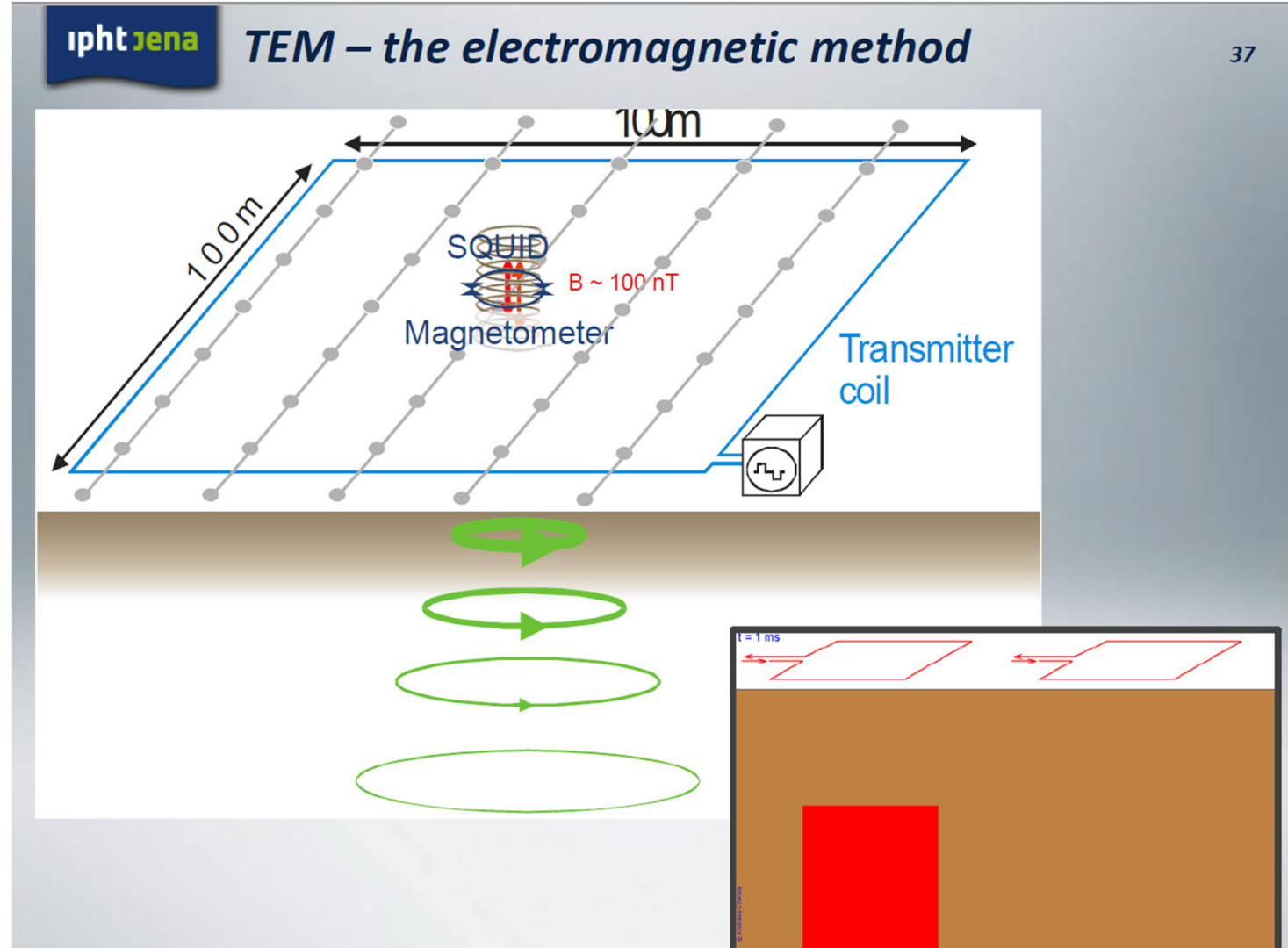


FIG. 39. (Color online) Output of HTS planar gradiometer flying over a commercial vehicle (arbitrary units). The gradiometer was inside a tail mounted stinger on a Cessna Caravan airplane.

Fagaly, Rev. Sci. Instr. 2006, doi: 10.1063/1.2354545

Transient Electromagnetic Pulses (MAD)





TRISTAN Technologies



Jülicher SQUID GmbH



SIMIT and Jilin Univ.



Supracon: JESSY DEEP HTS



Supracon: JESSY DEEP LTS



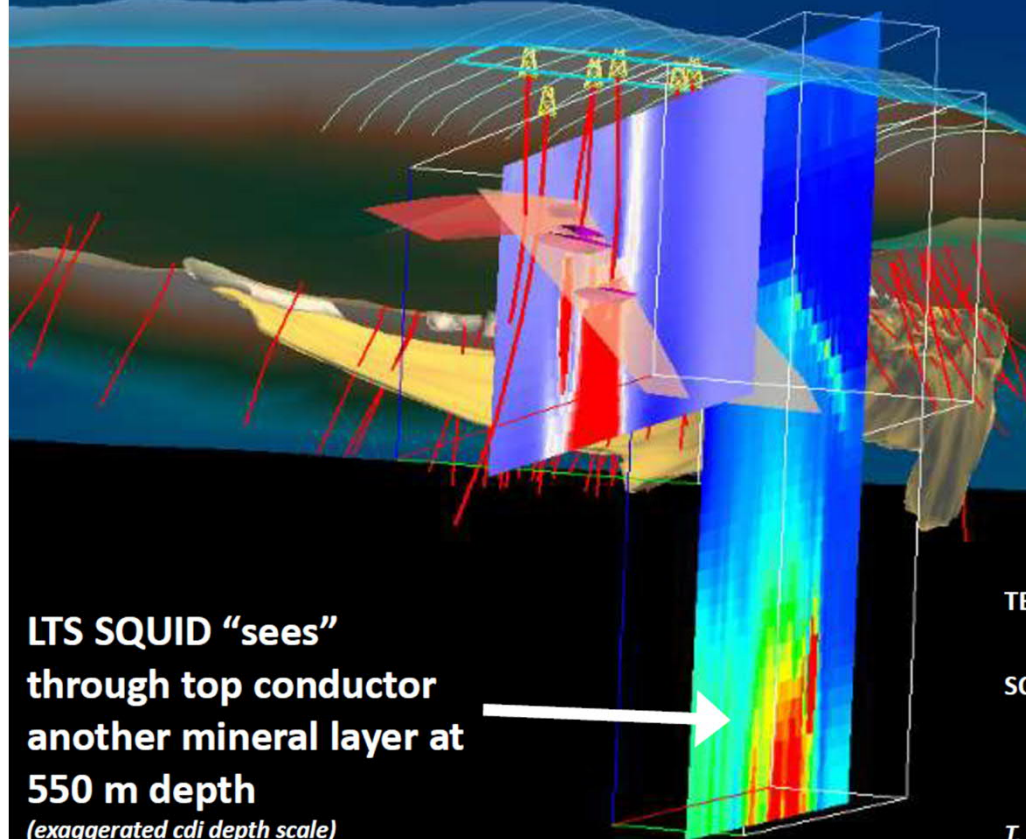
CSIRO: LandTEM

ISTEC: SQUITEM-3

Hato, SUST 26 (2013) 115003



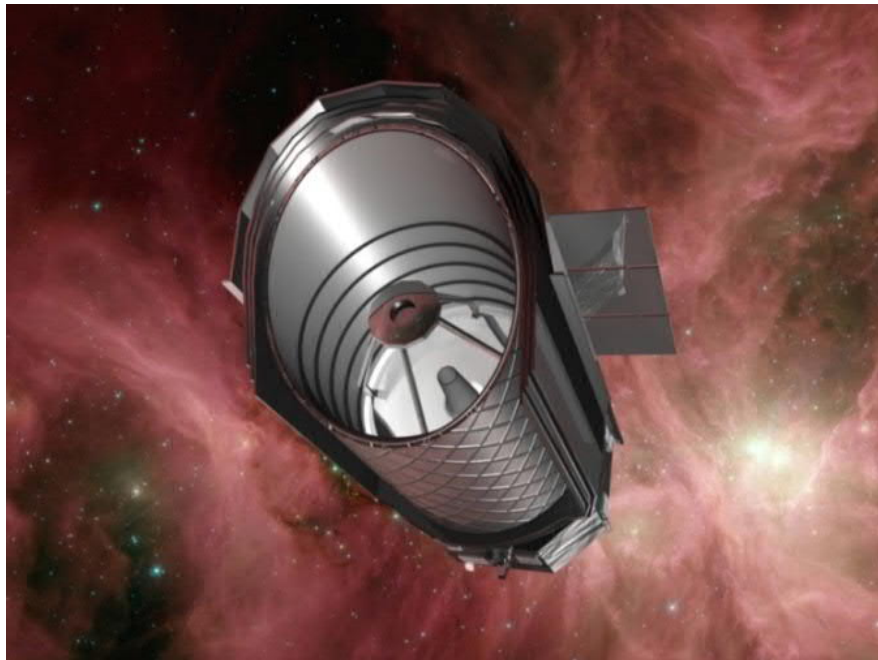
T. leRoux and J. Macnae, exploration 07



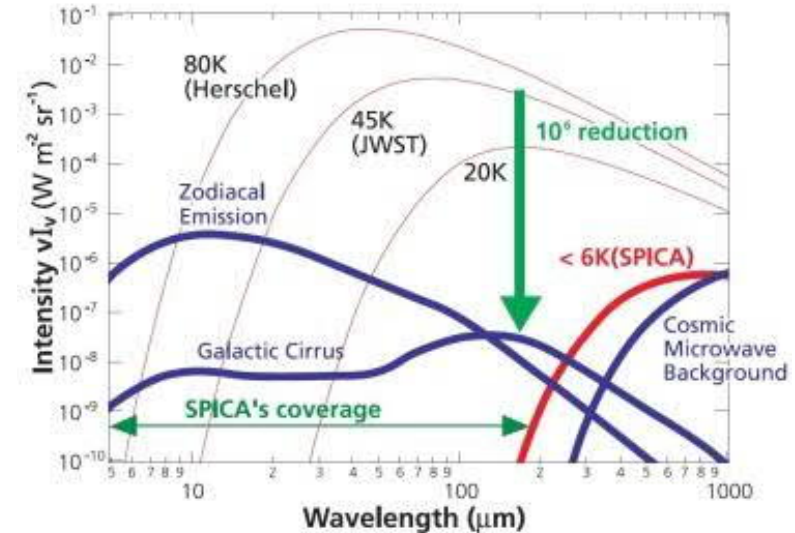


TES detector multiplexing

SPICA mission: SAFARI instrument



Jackson et al, IEEE Trans. THz Tech. 2 12 (2012)

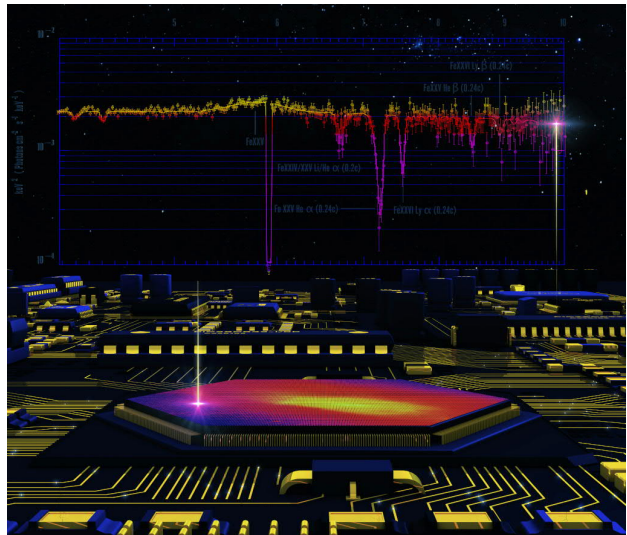


SAFARI instrument

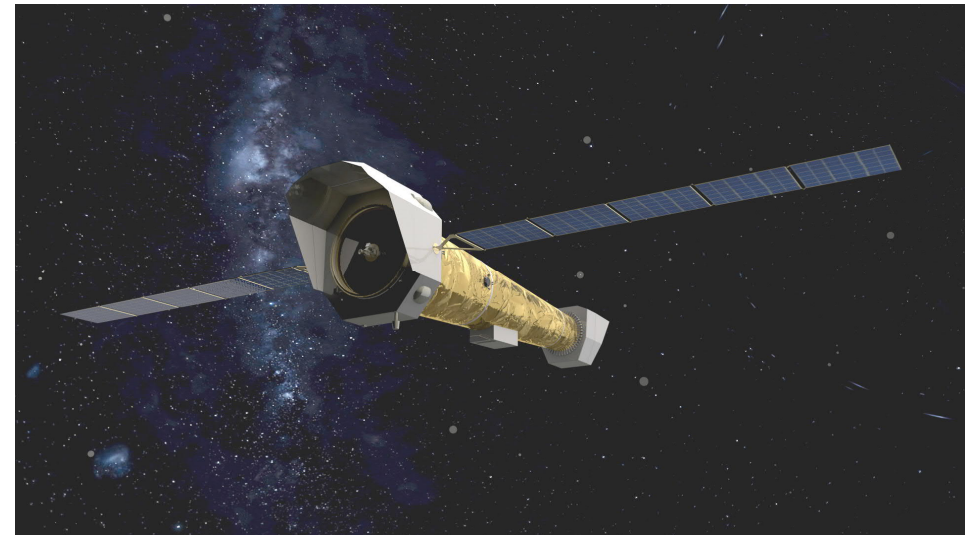
- TES bolometer array
- 3528 pixels
- SW 34-56μm, MW 54-89μm, LW1 87-143μm, LW2 140-230μm
- FDM readout

ATHENA mission

Advanced Telescope for High-energy Astrophysics



X-IFU instrument: 3168-pixel array of superconducting X-ray calorimeters at $T = 50\text{ mK}$



<http://http://x-ifu.irap.omp.eu/>
<https://www.youtube.com/watch?v=mOf6WIDmi30>

Beamline instruments

Beamline instruments



Multiplexing: remainder of linear algebra

Take detector signals $s_1(t), s_2(t), s_3(t) \dots s_N(t)$ and band-limit so that
they are effectively constant $s_1, s_2, s_3 \dots s_N$

Multiplexing: remainder of linear algebra

Take detector signals $s_1(t), s_2(t), s_3(t) \dots s_N(t)$ and band-limit so that

they are effectively constant $s_1, s_2, s_3 \dots s_N$

Take an orthogonal set of basis functions $\langle \varphi_1 |, \langle \varphi_2 |, \langle \varphi_3 | \dots \langle \varphi_N |$ (fingerprints)



Multiplexing: remainder of linear algebra

Take detector signals $s_1(t), s_2(t), s_3(t) \dots s_N(t)$ and band-limit so that
they are effectively constant $s_1, s_2, s_3 \dots s_N$

Take an orthogonal set of basis functions $\langle \varphi_1 |, \langle \varphi_2 |, \langle \varphi_3 | \dots \langle \varphi_N |$ (fingerprints)

Multiply signals with basis functions $s_1 \langle \varphi_1 |, s_2 \langle \varphi_2 |, s_3 \langle \varphi_3 | \dots s_N \langle \varphi_N |$



Multiplexing: remainder of linear algebra

Take detector signals $s_1(t), s_2(t), s_3(t) \dots s_N(t)$ and band-limit so that

they are effectively constant $s_1, s_2, s_3 \dots s_N$

Take an orthogonal set of basis functions $\langle \varphi_1 |, \langle \varphi_2 |, \langle \varphi_3 | \dots \langle \varphi_N |$ (fingerprints)

Multiply signals with basis functions $s_1 \langle \varphi_1 |, s_2 \langle \varphi_2 |, s_3 \langle \varphi_3 | \dots s_N \langle \varphi_N |$

Now signals can be summed $s_{tot}(t) = s_1 \langle \varphi_1 | + s_2 \langle \varphi_2 | + s_3 \langle \varphi_3 | \dots + s_N \langle \varphi_N |$

The total signal transferred from cryostat to room temperature over single wire



Multiplexing: reminder of linear algebra

Take detector signals $s_1(t), s_2(t), s_3(t) \dots s_N(t)$ and band-limit so that

they are effectively constant $s_1, s_2, s_3 \dots s_N$

Take an orthogonal set of basis functions $\langle \varphi_1 |, \langle \varphi_2 |, \langle \varphi_3 | \dots \langle \varphi_N |$ (fingerprints)

Multiply signals with basis functions $s_1 \langle \varphi_1 |, s_2 \langle \varphi_2 |, s_3 \langle \varphi_3 | \dots s_N \langle \varphi_N |$

Now signals can be summed $s_{tot}(t) = s_1 \langle \varphi_1 | + s_2 \langle \varphi_2 | + s_3 \langle \varphi_3 | \dots + s_N \langle \varphi_N |$

The total signal transferred from cryostat to room temperature over single wire

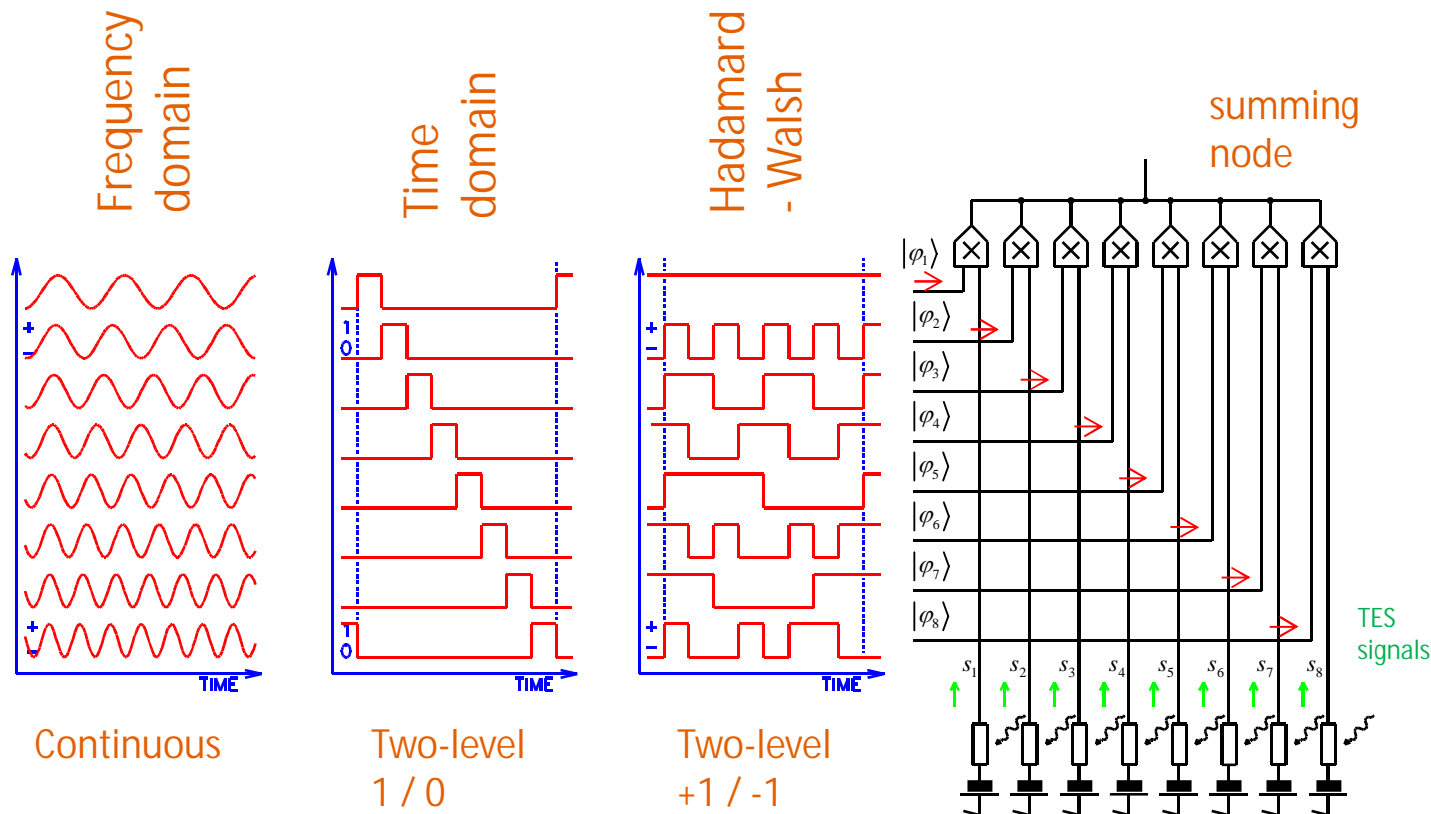
At room temperature:

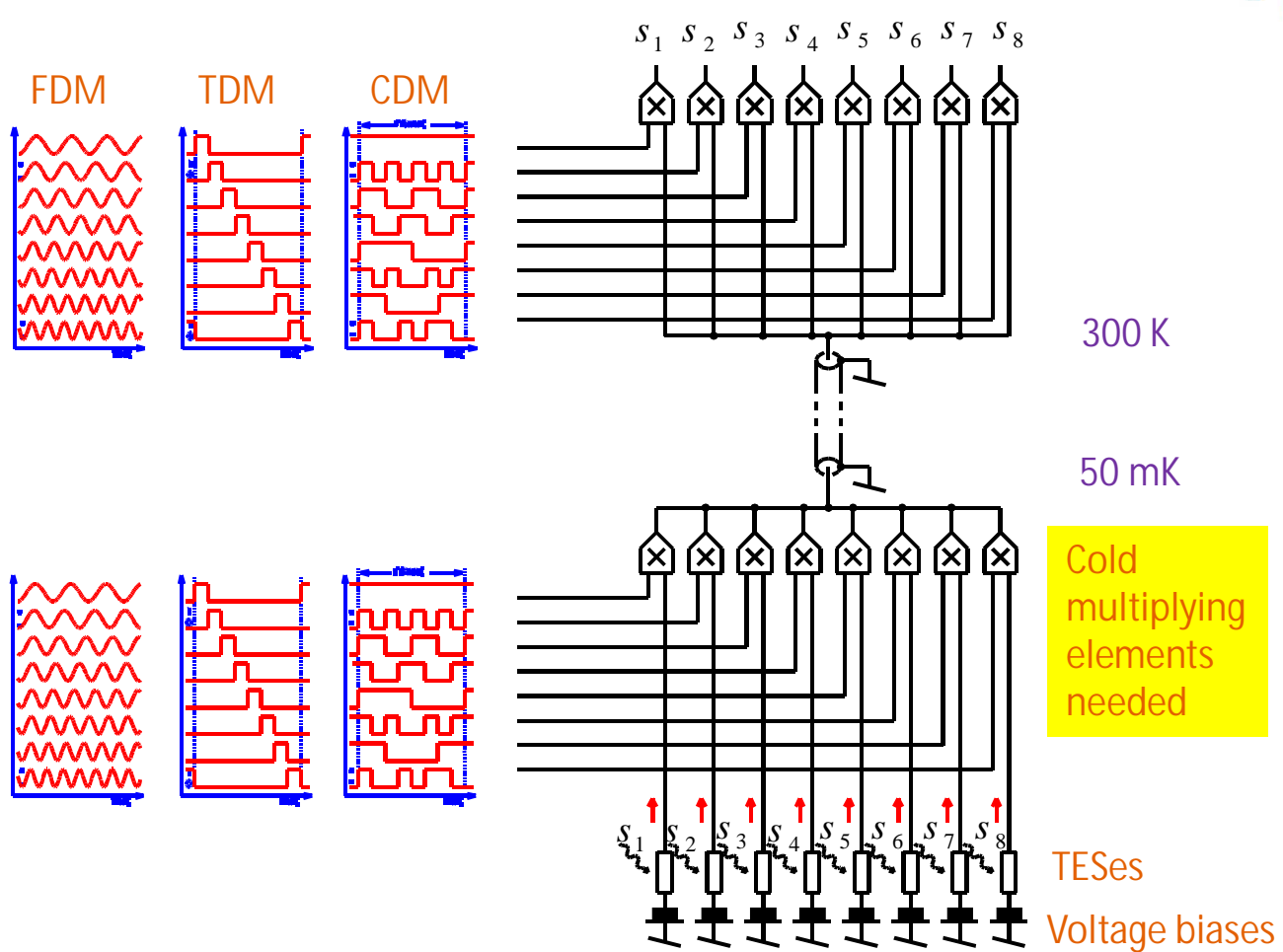
$$s_{tot}(t) |\varphi_1\rangle = (s_1 \langle \varphi_1 | + s_2 \langle \varphi_2 | + s_3 \langle \varphi_3 | \dots + s_N \langle \varphi_N |) |\varphi_1\rangle = s_1$$

$$s_{tot}(t) |\varphi_2\rangle = s_2$$

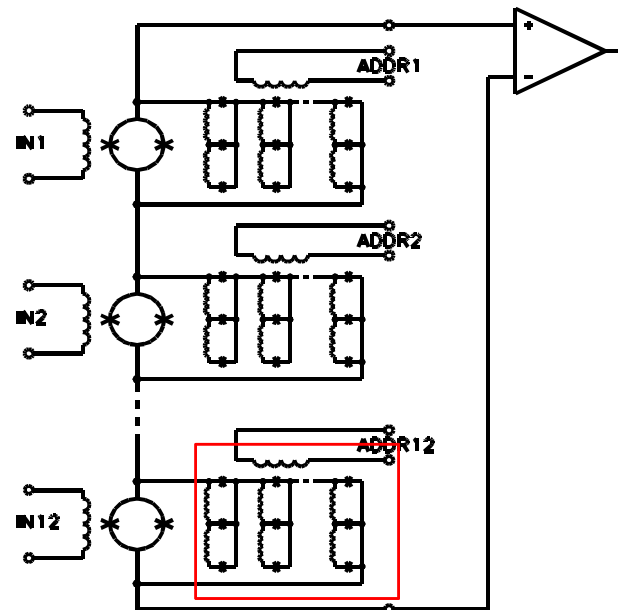
$$s_{tot}(t) |\varphi_3\rangle = s_3 \quad \text{etc.}$$

Orthogonal basis sets for multiplexing

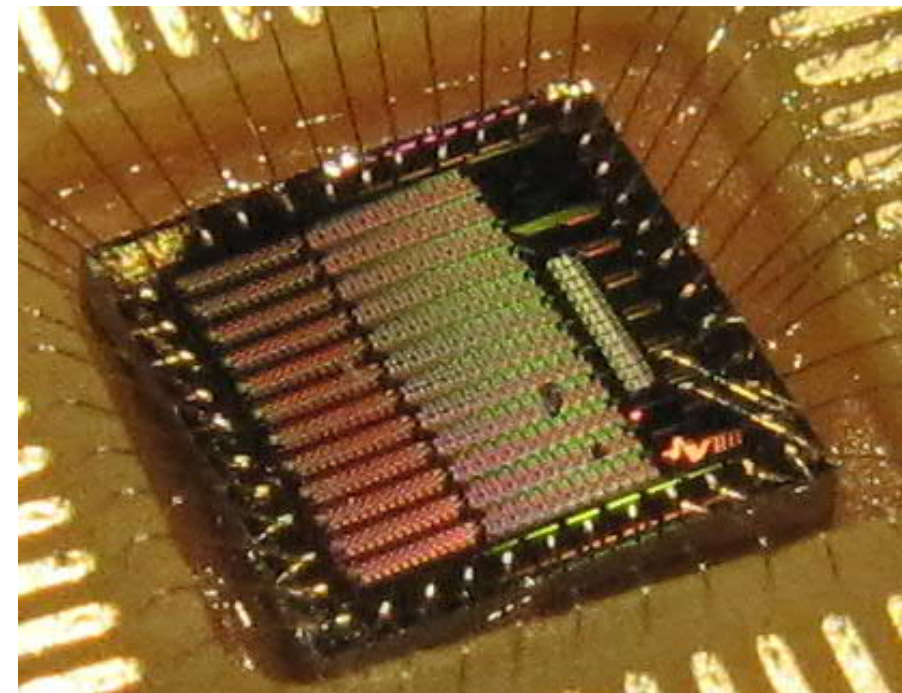




12-channel Beyer-style time domain MUX using voltage-state Zappe switches



Array of flux-controlled superconductive-normal (Zappe) switches: short-circuit all but one amplifier SQUID



doi:10.1088/1742-6596/507/4/042003

40-channel TD-MUX for ATHENA

IEEE TRANSACTIONS ON APPLIED SUPERCONDUCTIVITY, VOL. 29, NO. 5, AUGUST 2019

2101005

Demonstration of Athena X-IFU Compatible 40-Row Time-Division-Multiplexed Readout

Malcolm Durkin , Joseph S. Adams, Simon R. Bandler, James A. Chervenak, Saptarshi Chaudhuri, Carl S. Dawson, Edward V. Denison, William B. Doriese , Shannon M. Duff, Fred M. Finkbeiner , Connor T. FitzGerald, Joseph W. Fowler, Johnathon D. Gard, Gene C. Hilton, Kent D. Irwin, Young Il Joe, Richard L. Kelley, Caroline A. Kilbourne , Antoine R. Minissi, Kelsey M. Morgan , Galen C. O’Neil, Christine G. Pappas, Frederick S. Porter, Carl D. Reintsema, David A. Rudman, Kazuhiro Sakai, Stephen J. Smith, Robert W. Stevens, Daniel S. Swetz, Paul Szypryt, Joel N. Ullom, Leila R. Vale, Nicholas A. Wakeham , Joel C. Weber, and Betty A. Young

Abstract—Time-division multiplexing (TDM) is the backup readout technology for the X-ray Integral Field Unit (X-IFU), a 3168-pixel X-ray transition-edge sensor (TES) array that will provide imaging spectroscopy for European Space Agency’s Athena satellite mission. X-IFU design studies are considering readout with a multiplexing factor of up to 40. We present data showing 40-row TDM readout (32 TES rows + 8 repeats of the last row) of TESs that are of the same type as those being planned for X-IFU, using measurement and analysis parameters within the ranges specified for X-IFU. Single-column TDM measurements have best-fit energy resolution of (2.03 ± 0.01) eV for Ti K α and (2.40 ± 0.01) eV for Co K α . The degradation due to the multiplexed readout ranges from 0.1 eV at the lower end of the energy range to 0.5 eV at the higher end. The demonstrated performance meets X-IFU’s energy-resolution and energy-range requirements. True 40-row TDM readout, without repeated rows, of kilopixel scale arrays of X-IFU-like TESs is now under development.

Index Terms—Transition-edge sensors, superconducting quantum interference devices, multiplexed readout, athena satellite.

I. INTRODUCTION

Due to their combination of high collecting efficiency [1] and high energy-resolution [2], arrays of transition-edge-

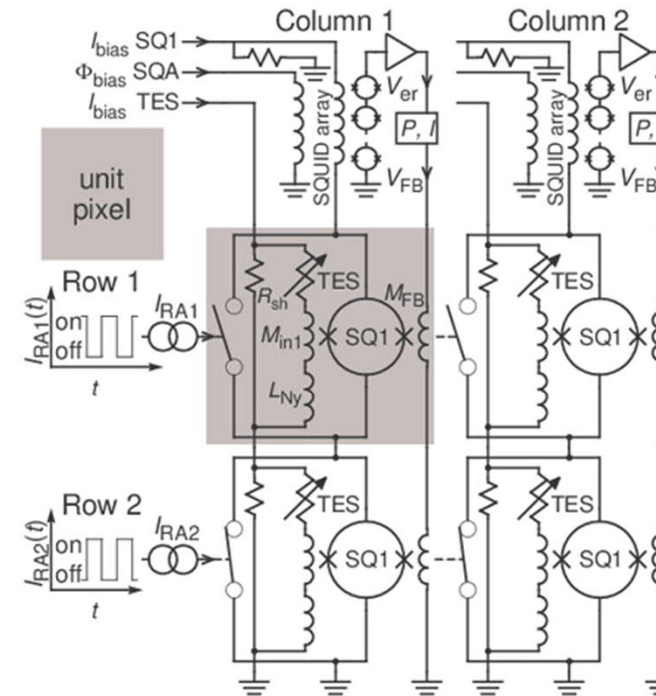


Fig. 1. Schematic of 2-column \times 2-row TDM. Each dc-biased TES is read out by a first stage SQUID amplifier (SQ1) via inductive coupling (M_{in1}). A row of

14-channel FD-MUX demonstration for ATHENA

Journal of Low Temperature Physics
<https://doi.org/10.1007/s10909-020-02351-3>



Progress in the Development of Frequency-Domain Multiplexing for the X-ray Integral Field Unit on Board the Athena Mission

H. Akamatsu¹ · L. Gottardi¹ · J. van der Kuur² · C. P. de Vries¹ · M. P. Bruijn¹ · J. A. Chervenak³ · M. Kiviranta⁴ · A. J. van den Linden¹ · B. D. Jackson^{1,2} · A. Miniussi³ · K. Ravensberg¹ · K. Sakai³ · S. J. Smith³ · N. Wakeham³

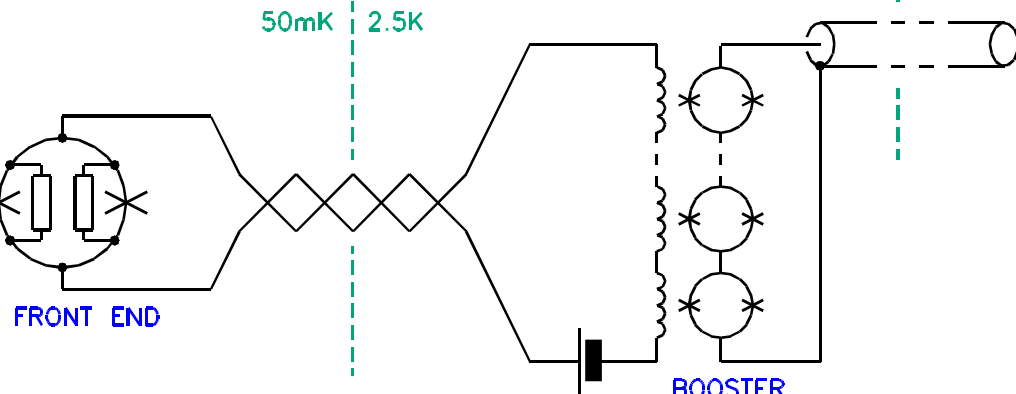
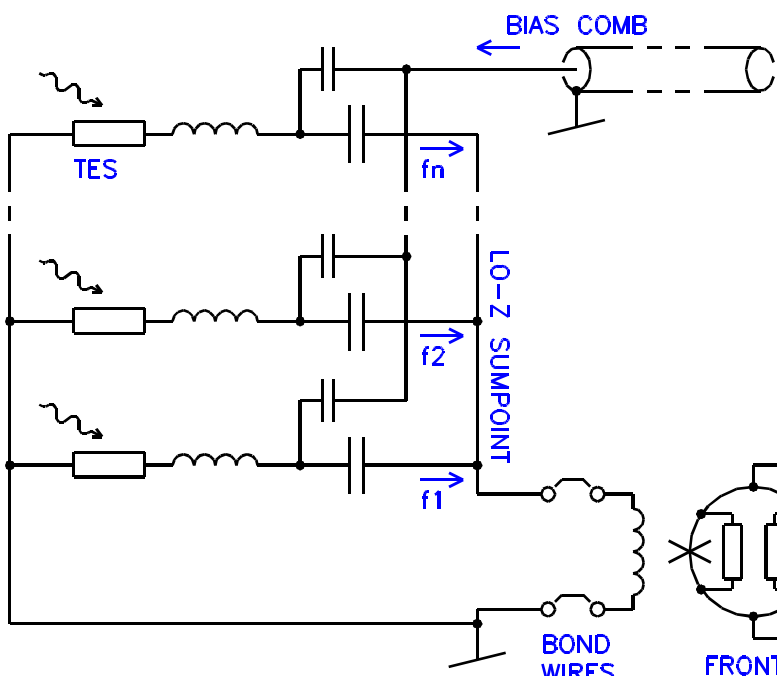
Received: 20 August 2019 / Accepted: 14 January 2020
 © Springer Science+Business Media, LLC, part of Springer Nature 2020

Abstract

Frequency-domain multiplexing (FDM) is the baseline readout system for the X-ray

2.5K

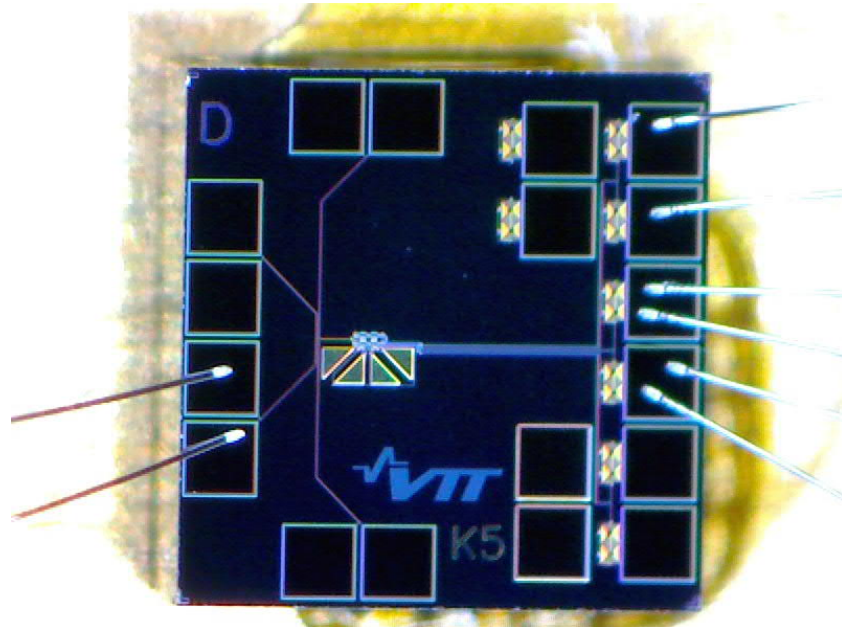
300K



14-channel FD-MUX demonstration for ATHENA

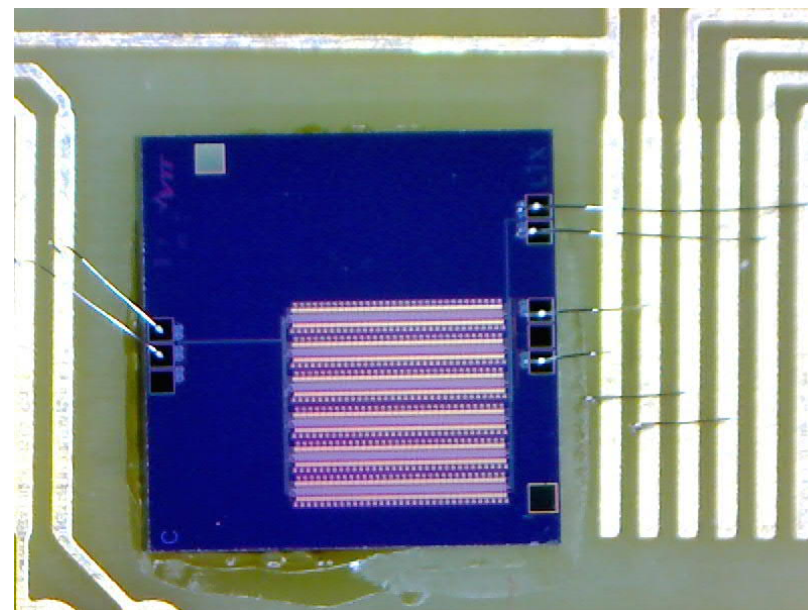
VTT

Front-end: K5 and K5B



Booster: L1 and L1X

- 3 x 128 –SQUID array



176-channel FD-MUX for SPICA

Journal of Low Temperature Physics (2020) 199:723–729
<https://doi.org/10.1007/s10909-020-02399-1>



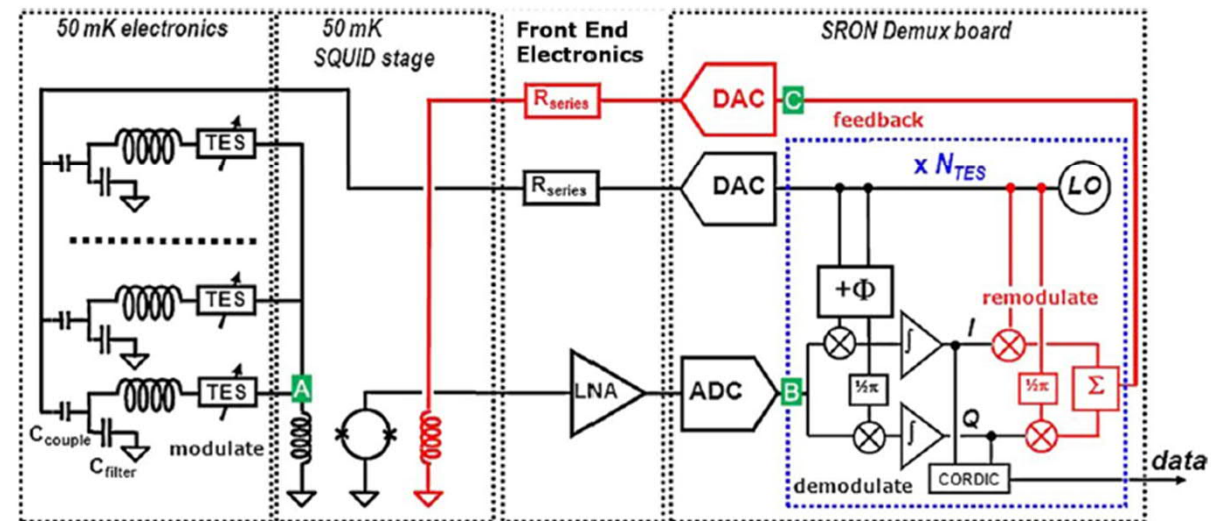
SQUID Noise in a 176-Pixel FDM Demonstrator for the SAFARI Far-Infrared Spectrometer

Michael D. Audley¹ · Qian Wang^{1,2} · Richard A. Hijmering³ ·
 Pourya Khosropanah³ · Gert de Lange¹ · Anton J. van der Linden³ ·
 Marcel L. Ridder³ · Emanuele Taralli³

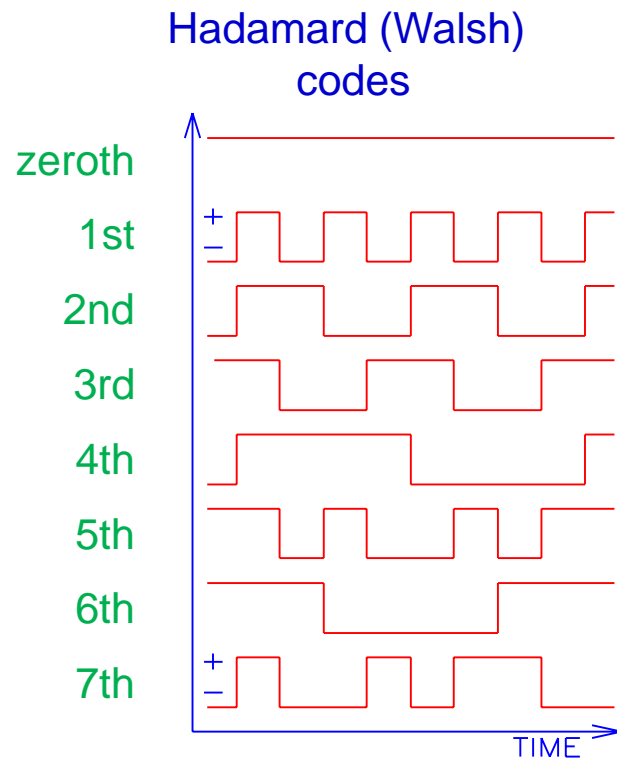
Received: 20 August 2019 / Accepted: 8 February 2020 / Published online: 17 February 2020
 © Springer Science+Business Media, LLC, part of Springer Nature 2020

Abstract

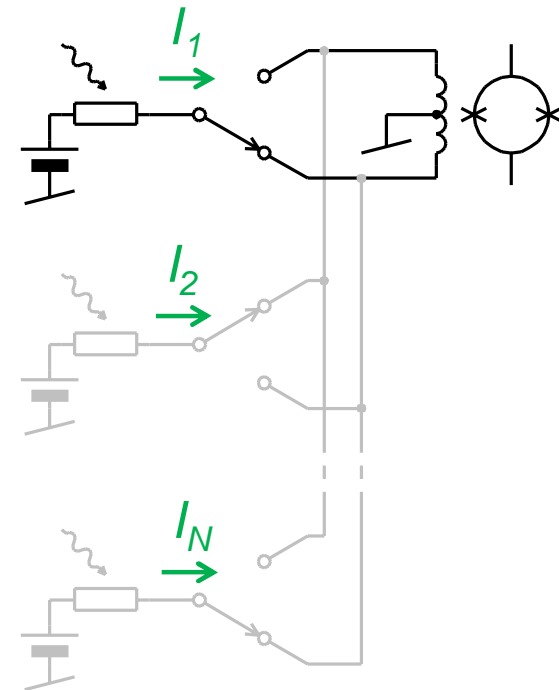
We are developing the frequency-domain multiplexing (FDM) readout for the SAFARI far-infrared spectrometer on board the SPICA space observatory.



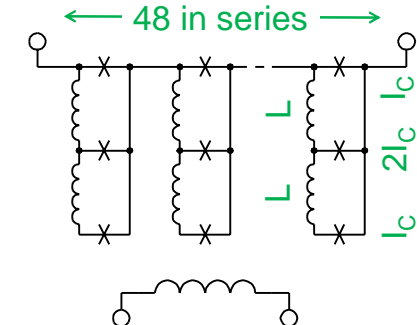
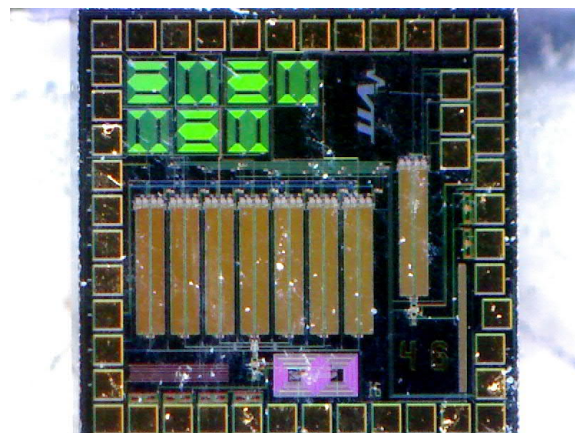
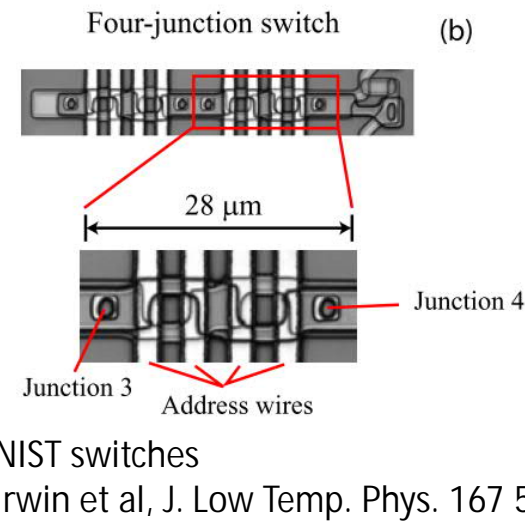
Code domain multiplexing



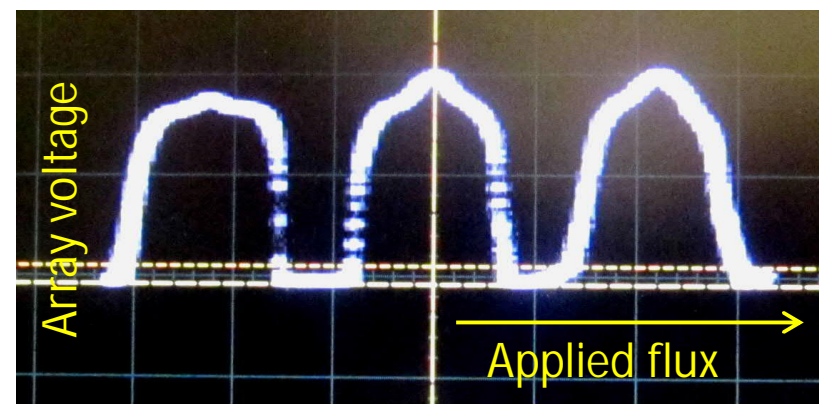
Codes are **bipolar two-level**
⇒ multiplication by a
commutating switch



Code domain multiplexing



VTT/Jena switches, E-SQUID project 2010-14, unpublished



Code domain multiplexing

APPLIED PHYSICS LETTERS 109, 112604 (2016)

Code-division-multiplexed readout of large arrays of TES microcalorimeters

K. M. Morgan,^{1,a)} B. K. Alpert,¹ D. A. Bennett,¹ E. V. Denison,¹ W. B. Doriese,¹ J. W. Fowler,¹ J. D. Gard,¹ G. C. Hilton,¹ K. D. Irwin,² Y. I. Joe,¹ G. C. O'Neill,¹ C. D. Reintsema,¹ D. R. Schmidt,¹ J. N. Ullom,¹ and D. S. Szwetz^{1,b)}

¹National Institute of Standards and Technology, Boulder, Colorado 80305, USA

²Stanford University, Palo Alto, California 94305, USA

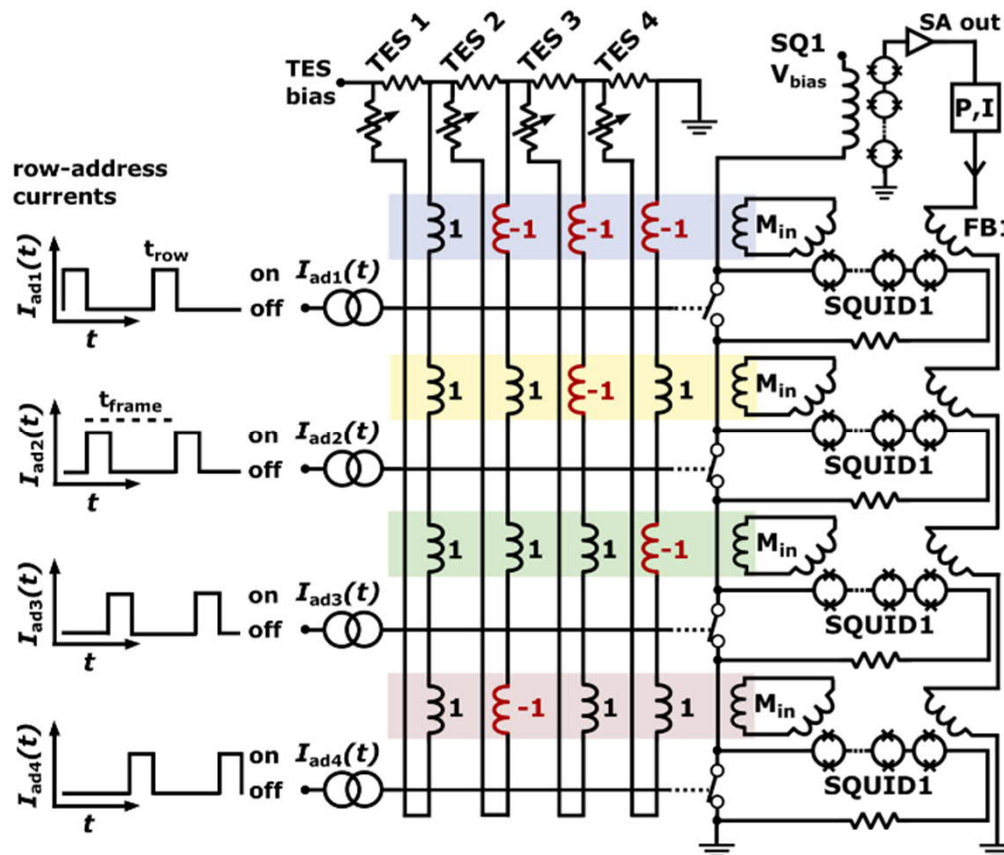
(Received 28 July 2016; accepted 27 August 2016; published online 15 September 2016)

Code-division multiplexing (CDM) offers a path to reading out large arrays of transition edge sensor (TES) X-ray microcalorimeters with excellent energy and timing resolution. We demonstrate the readout of X-ray TESs with a 32-channel flux-summed code-division multiplexing circuit based on superconducting quantum interference device (SQUID) amplifiers. The best detector has energy resolution of 2.28 ± 0.12 eV FWHM at 5.9 keV and the array has mean energy resolution of 2.77 ± 0.02 eV over 30 working sensors. The readout channels are sampled sequentially at 160 ns/row, for an effective sampling rate of $5.12 \mu\text{s}/\text{channel}$. The SQUID amplifiers have a measured flux noise of $0.17 \mu\Phi_0/\sqrt{\text{Hz}}$ (non-multiplexed, referred to the first stage SQUID). The multiplexed noise level and signal slew rate are sufficient to allow readout of more than 40 pixels per column, making CDM compatible with requirements outlined for future space missions. Additionally, because the modulated data from the 32 SQUID readout channels provide information on each X-ray event at the row rate, our CDM architecture allows determination of the arrival time of an X-ray event to within 275 ns FWHM with potential benefits in experiments that require detection of near-coincident events.

Published by AIP Publishing. [<http://dx.doi.org/10.1063/1.4962636>]

A transition-edge sensor (TES) microcalorimeter is a superconducting thin film in which the superconducting-to-

penalty and samples all sensors in a column simultaneously. However, the LC components can be physical





A few more exotic applications

Josephson Travelling Wave Parametric Ampl's



Early work at VTT, doi:

PNAS

Dynamical Casimir effect in a Josephson metamaterial

Pasi Lähteenmäki^{a,1}, G. S. Paraoanu^a, Juha Hassel^b, and Pertti J. Hakonen^a

^aO. V. Lounasmaa Laboratory, Aalto University, 00076, Espoo, Finland; and ^bVTT Technical Research Centre of Finland, 02044, Espoo, Finland

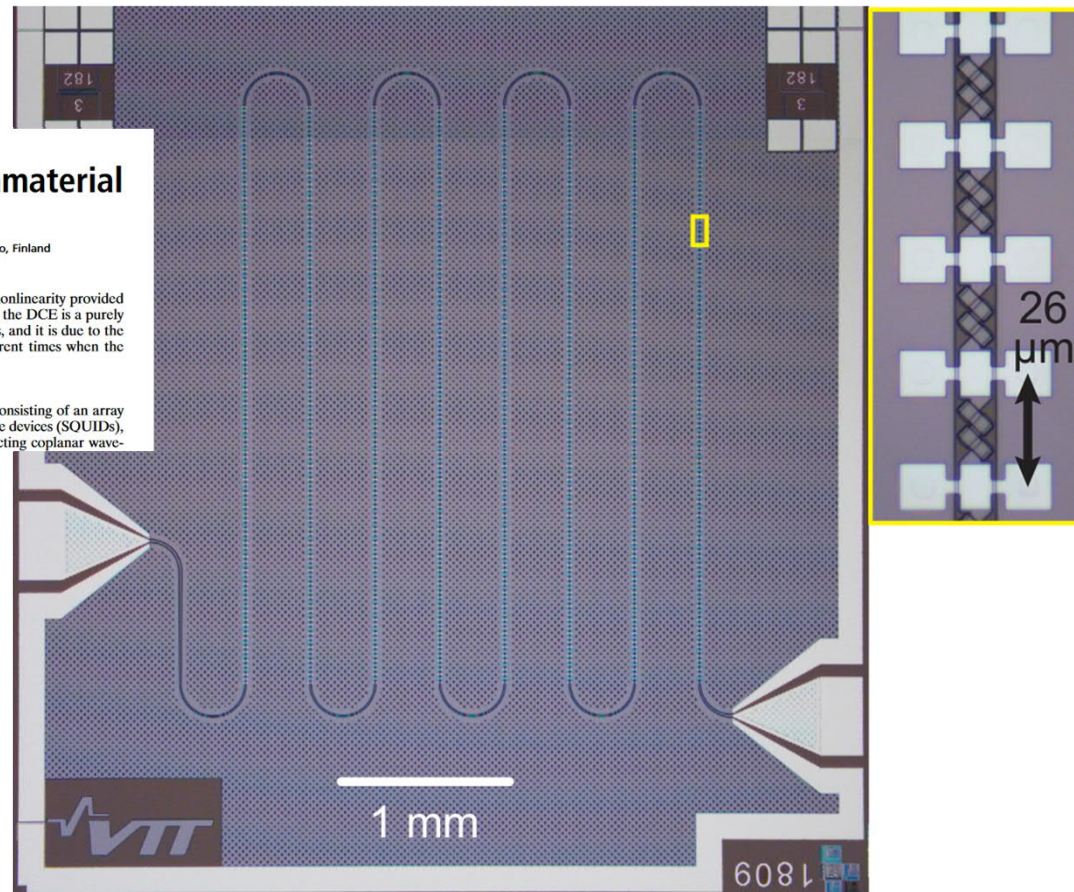
Edited by Steven M. Girvin, Yale University, New Haven, CT, and approved January 8, 2013 (received for review August 13, 2012)

The zero-point energy stored in the modes of an electromagnetic cavity has experimentally detectable effects, giving rise to an attractive interaction between the opposite walls, the static Casimir effect. A dynamical version of this effect was predicted to occur when the vacuum energy is changed either by moving the walls of the cavity or by changing the index of refraction, resulting in the conversion of vacuum fluctuations into real photons. Here, we demonstrate the dynamical Casimir effect using a Josephson metamaterial embedded in a microwave cavity at 5.4 GHz. We modulate the effective length of the cavity by flux-biasing the metamaterial

pumped crystals (21, 22) or the equivalent nonlinearity provided by Josephson junctions (23–25). In contrast, the DCE is a purely dynamical effect, occurring in linear systems, and it is due to the mismatch between the field modes at different times when the vacuum is perturbed fast enough.

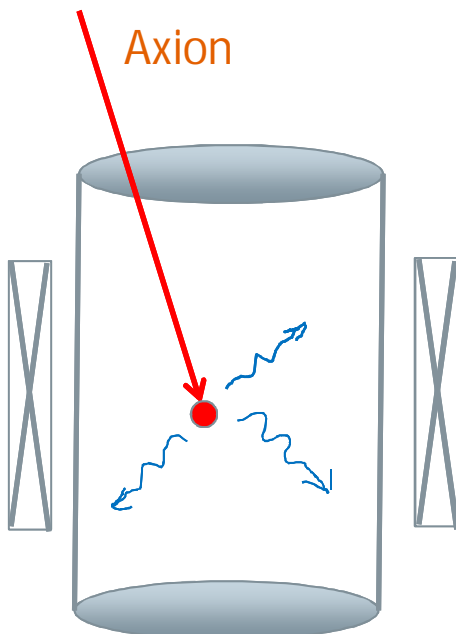
Experimental Setup

Our medium is a Josephson metamaterial consisting of an array of 250 superconductive quantum interference devices (SQUIDs), which form the signal line of a superconducting coplanar wave-

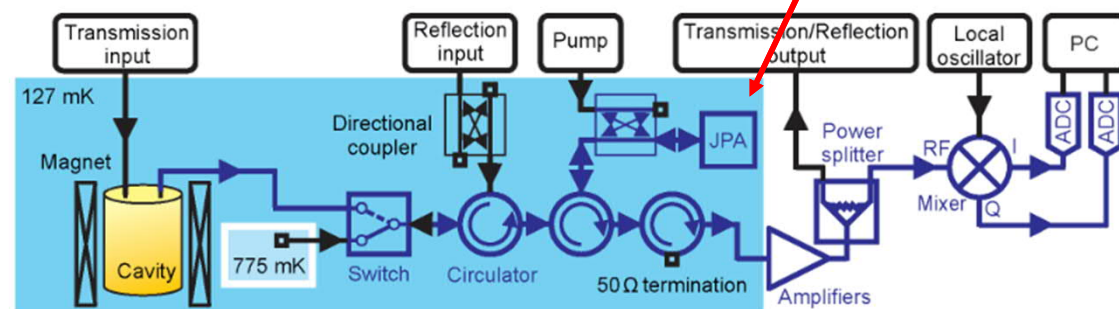


SEM picture arXiv:2009.03010

Axions: dark mass search

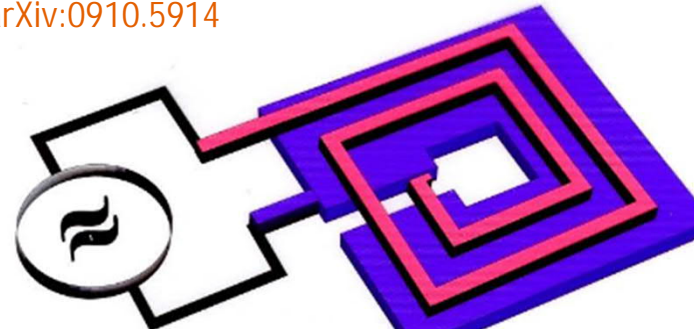


HAYSTAC experiment
arXiv:1610.02580

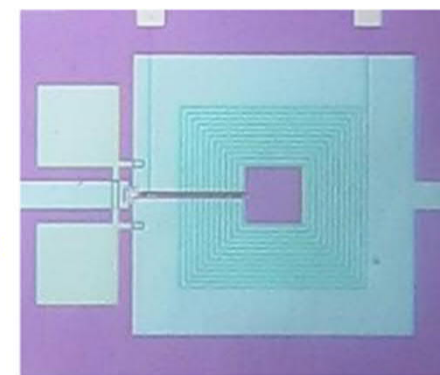


Josephson Parametric Amplifier @5.8 GHz

ADMX experiment
arXiv:0910.5914

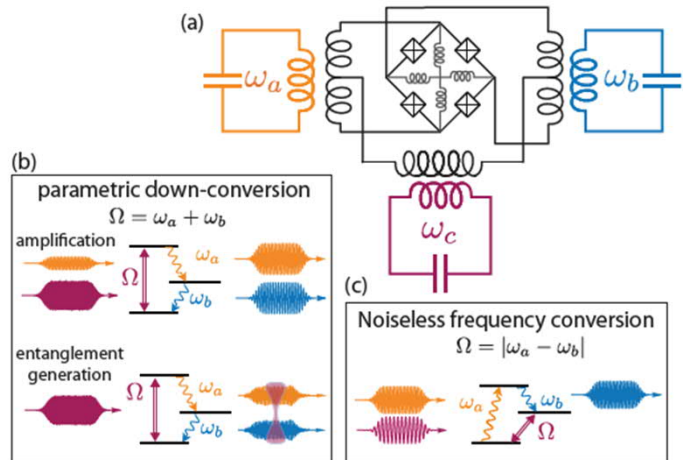


Microstrip SQUID @600 MHz or 0-200 MHz

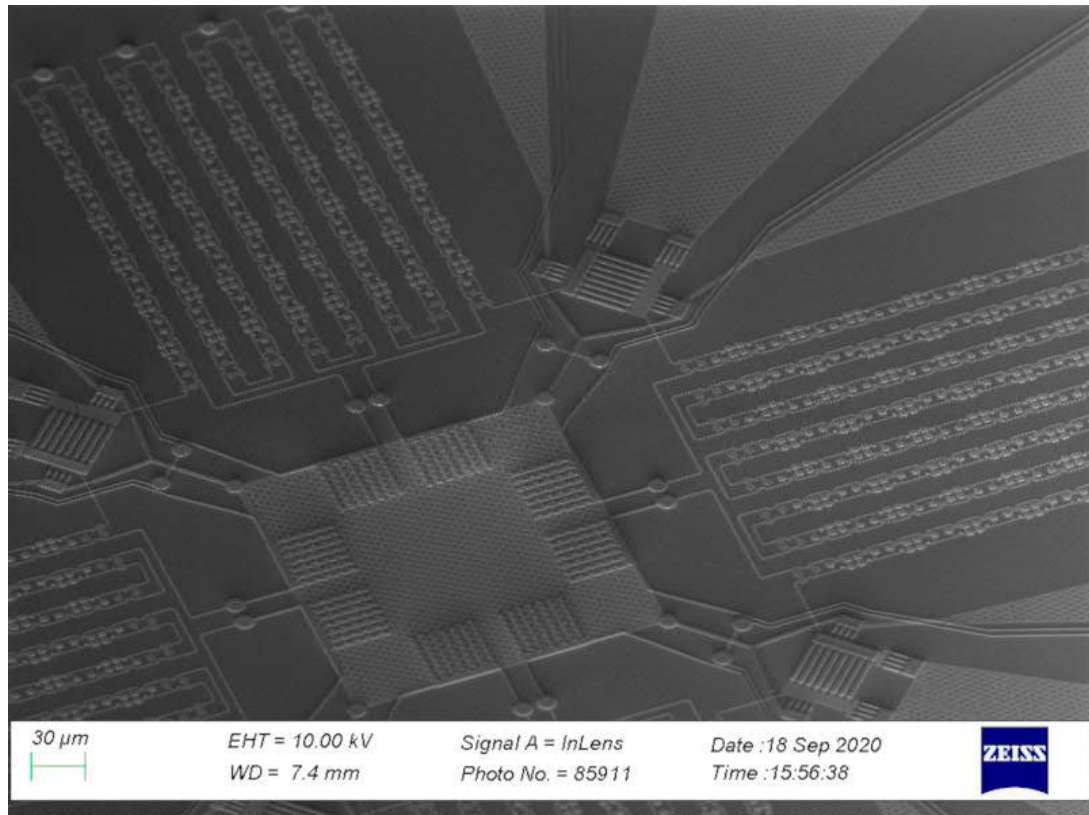


<https://www.quantamagazine.org/how-axions-may-explain-times-arrow-20160107/>
https://en.wikipedia.org/wiki/Axion_Dark_Matter_Experiment

Josephson Parametric Converter



Emmanuel Flurin, PhD thesis



SEM picture
from QuMics project
<http://qmics.wmi.badw.de/>

Thank you for listening

- Magnetoencephalography
- Ultra-low field Magnetic Resonance Imaging
- Geomagnetism
- Multiplexing Transition Edge Sensors
- A few more exotic applications